Hydrogenation of Quinoline by Rhodium Catalysts Modified with the Tripodal Polyphosphine Ligand $MeC(CH_2PPh_2)_3$

by **Claudio Bianchini***, **Pierluigi Barbaro**, **Michela Macchi**, **Andrea Meli**, and **Francesco Vizza**

Istituto per lo Studio della Stereochimica ed Energetica dei Composti di Coordinazione, ISSECC-CNR, Via J. Nardi 39, I-50132 Firenze (Tel.: +39-055-245-990; fax: +39-055-247-8366; e-mail: bianchin@fi.cnr.it)

Dedicated to the late Professor *Luigi M. Venanzi*, a friend, a master, and a pioneer in the organometallic chemistry of polydentate ligands

As part of our modelling studies of the hydrodenitrogenation of N-heterocycles contained in raw oil materials, we investigated the selective hydrogenation of quinoline to 1,2,3,4-tetrahydroquinoline by rhodium catalysts modified with the tripodal polyphosphane ligand $MeC(CH_2PPh_2)_3$. Experiments in standard autoclaves and in high-pressure sapphire NMR tubes, kinetic and isotope labelling studies, and independent reactions with isolated compounds have contributed to the elucidation of the catalytic mechanism as well as identification of the electronic requisites of the metal catalyst for selective and efficient hydrogenation.

1. Introduction. – Heteroatoms are currently removed from fossil fuels under hydro-treating conditions in the presence of heterogeneous catalysts that must be efficacious for four main chemical processes: hydrodesulfurization (HDS), hydrodenitrogenation (HDN), hydrodeoxygenation (HDO), and hydrodemetallation (HDM) [1][2]. In actual refinery reactors, HDN (*Eqn. 1*) occurs simultaneously to all the other hydro-treating processes, but the reaction parameters are optimized for the HDS reaction (*Eqn. 2*), and, therefore, the experimental conditions and the catalysts employed are not specifically optimized for HDN, which requires longer reaction times as well as higher temperature and H_2 pressure to occur as efficiently as HDS [1][3].

$$C_aH_bN + c\ H_2 \rightarrow NH_3 + C_aH_d \quad \text{Hydrodenitrogenation (HDN)} \tag{1}$$

$$C_aH_bS + c\ H_2 \rightarrow H_2S + C_aH_d \quad \text{Hydrodesulfurization (HDS)} \tag{2}$$

Nitrogen in petroleum and coal is contained in various organic compounds, including polyaromatic heterocycles, aliphatic and aromatic amines, and nitriles. The latter are in low quantity, and their degradation is efficiently performed under hydro-treating conditions with application of commercial catalysts, while the aromatic heterocycles, *e.g.*, quinolines, pyridines, pyrroles, and indoles, are much more difficult to degrade even than fused-ring thiophenes [1][3].

A relatively detailed mechanistic picture of the HDN of quinoline (Q) has been obtained from the combined efforts of heterogeneous and homogeneous studies. The former have been useful in rationalizing product distributions, kinetics, and selectivities, whereas homogeneous modelling studies have contributed to the elucidation of

bonding modes and reactivity of coordinated Q, the elementary steps of its metal-catalyzed hydrogenation, and the insertion of metal centers into either C–N bond [1][3–15].

Quinoline may interact with the metal sites in two principal modes: *end-on* through the N-atom and *side-on* through either ring or the C=N bond [3]. However, in the absence of steric congestion provided by α-substituents, the N-atom is used preferentially for interaction with the catalyst.

The principal reaction pathways [1][3][4] proposed for the HDN of Q are shown in *Scheme 1*. The most efficient reaction would proceed *via* the step sequence *a*) → *b*) → *c*), which does not involve the hydrogenation of the carbocyclic ring and, therefore, consumes less H_2 than any other path, and yields fuels with a higher octane rating due the residual aromaticity in the denitrogenated products. Most of Q, however, undergoes HDN over conventional catalysts *via* the alternative sequence of steps *a*) → *d*) → *e*) → *f*), which involves the hydrogenation of both rings and, therefore, consumes twice as much H_2 to give either propylcyclohexane or ethylcyclohexane. The hydrogenation of the heterocyclic ring is necessary to reduce the high energy required to cleave the C–N bond that, in a typical *N*-heterocycle, is close to that of a C=N bond [3a]. Since the most efficacious HDN catalysts are also good hydrogenation catalysts of the heterocyclic ring [1][3], a deep understanding of the elementary steps involved in the hydrogenation mechanism of Q is of utmost importance for designing improved HDN catalysts, possibly to drive the reaction through the pathway *a*) → *b*) → *c*). To this purpose, homogeneous modelling studies with soluble metal catalysts might be very helpful, especially to obtain specific information on the optimal electronic and steric properties of the metal promoters and on the most appropriate reaction conditions for selective hydrogenation.

Scheme 1

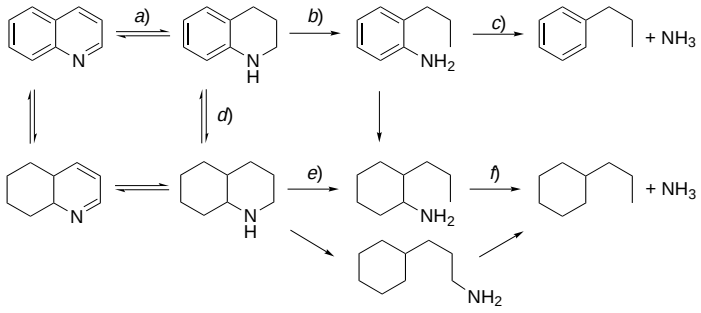

The first example of hydrogenation of Q to 1,2,3,4-tetrahydroquinoline (THQ) with a soluble metal catalyst was reported by *Jardine* and *McQuillin* in 1970 [16]. Since then, various transition metals (Mn, Fe, Co, Rh, Ru, Os) have been found capable of forming catalysts for the selective conversion of Q to THQ in different phase-variation systems that range from being truly homogeneous [4][7a,i,k,l][9a–e,g], to aqueous-biphasic [4][17] to heterogeneous single-site [4][18] (*Scheme 2*). In contrast to the relative abundance of catalysts, very few mechanistic and kinetic studies of the selective hydrogenation of Q have been reported so far [4][7a,i][9c,e]. Accordingly, the relative

kinetic relevance of each catalytic step and the optimal catalyst composition to give high productivity and selectivity are issues that need further investigation.

Scheme 2

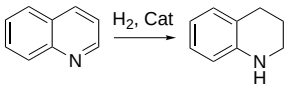

As part of ongoing studies of HDS catalysis by phosphane-modified late-transition-metal catalysts [19], we have recently discovered that the tripodal tridentate ligand $MeC(CH_2PPh_2)_3$ (triphos) forms, in combination with Rh and Ru, either $16e^-$ or $14e^-$ fragments of the formulas $[M(H)(triphos)]^n$ ($M = Rh$, $n = 0$; $M = Ru$, $n = -1, +1$) and $[Rh(H)_2(triphos)]^+$. Irrespective of the metal, the Rh^I and Ru^0 $16e^-$ fragments promote exclusively the hydrogenolysis reaction of thiophenes to thiols (C–S insertion followed by hydrogenation), while the $14e^-$ Ru^{II} complex is a selective catalyst for hydrogenation to thioethers. No reaction was observed between the $16e^-$ Rh^{III} fragment $[Rh(H)_2(triphos)]^+$ and thiophenes, which was attributed to the low propensity of Rh^{III} to bind *S*-heterocycles [20][21].

M = Rh, *n* = 0
M = Ru, *n* = –1, +1

Since HDS and HDN catalysis can occur simultaneously over the surface of heterogeneous catalysts, we decided to investigate systematically the hydrogenation of N-heterocycles with the same triphos precursors employed for the hydrogenation and/or hydrogenolysis of thiophenes. In this paper, we show that the selective hydrogenation of Q to THQ can be achieved effectively in homogeneous phase with catalyst precursors that generate the fragment $[Rh(H)_2(triphos)]^+$. The results obtained confirm that hydro-treating catalysts must contain metal sites with variable coordination numbers and variable oxidation states to be efficient for both HDS and HDN.

2. Results. – 2.1. *The Catalyst Precursors and Their Transformation in Hydrogen Atmosphere.* 2.1.1. *Hydrogenation in Tetrahydrofuran* (THF). From a formal viewpoint, both $[Rh(DMAD)(triphos)]PF_6$ (**1**) (DMAD = dimethyl acetylenedicarboxylate (dimethyl but-2-ynedioate)) [21d][22a] and $[Rh(S(C_6H_4)CH{=}CH_2\text{-}\kappa C^{1',2'},\kappa S)(triphos)]$ (**2**) [21j] contain Rh^I metal ions that are oxidized to Rh^{III} upon oxidative addition of H_2 (*Scheme 3*) [21][22]. In THF, both **1** and **2** behave as precursors to the $16e^-$ fragments $[Rh(H)_2(triphos)]^+$ and $[RhH(triphos)]$, respectively, which differ from each other in metal oxidation state and the number of terminal hydride ligands [23]. The Rh^I fragment can be trapped by nucleophiles to give stable five-coordinate complexes [24] or by electrophiles bearing C–H, C–S, and H–H bonds to give octahedral Rh^{III} insertion products [21–24].

Scheme 3

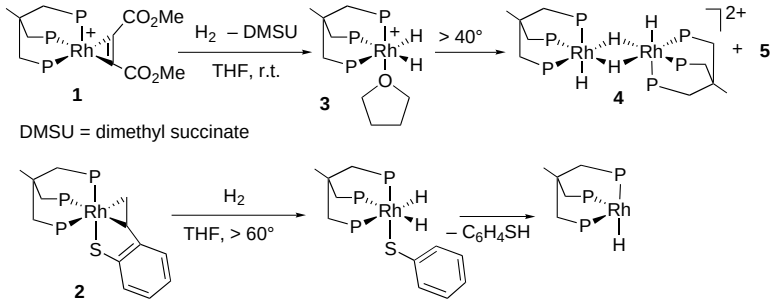

The plain transformation of [RhH(triphos)] into $[Rh(H)_2(triphos)]^+$, which can be stabilized by THF, to give $[Rh(H)_2(THF\text{-}\kappa O)(triphos)]^+$ (**3**) [25] can readily be achieved by reaction with a *Brønsted* acid. High-pressure NMR (HP-NMR) spectroscopy showed **3** to be thermally unstable in THF, where it is transformed into the binuclear compound $[\{Rh(H)\}_2(triphos\text{-}\kappa^3P)_2(\mu\text{-}H)_2](PF_6)_2$ (**4**) [23][25] and, to a much lesser extent, into a new hydride-containing triphos-Rh complex (**5**), whose structure is still obscure. In view of the propensity of Rh to form, in combination with triphos, various binuclear polyhydride complexes [23][25], it is very likely that **5** is also a binuclear species.

The hydrogenation of **2** to give free thiol C_6H_4SH and transient [RhH(triphos)] has already been reported [21a,f,g].

2.1.2. *Hydrogenation in THF in the Presence of Quinoline.* A sequence of $^{31}P\{^1H\}$-HP-NMR spectra relative to the hydrogenation of **1** in a (D_8)THF solution of Q (220 mM) is reported in *Fig. 1*. No transformation of the precursor took place until the tube was pressurized to 30 bar with H_2.

Within the time necessary to acquire the first spectrum at room temperature, the starting complex was completely converted to a mixture of Rh compounds, which have been unambiguously identified by either comparison with authentic specimens or a detailed spectroscopic analysis (*Fig 1, b*) (*Scheme 4*). The major products, which are featured by NMR signals in the chemical-shift regions from 31–35 ppm (coordinated phosphine atoms) and from −26– −28 ppm (free phosphine atoms), constitute a family of geometric isomers of the general formula $[Rh(Q\text{-}\kappa N)_2(triphos\text{-}\kappa^2P)]^+$ (**6a–c**). Occasionally, the formation of **6a–c** was accompanied by that of minor amounts of their phosphane oxide derivatives $[Rh(Q\text{-}\kappa N)_2(triphos{=}O\text{-}\kappa^2P)]^+$ (**6x–z**) (triphos=O = $(Ph_2PCH_2)_2C(Me)CH_2PPh_2O$) (*vide infra*). The Rh^{III} dihydride $[Rh(H)_2(Q\text{-}\kappa N)(triphos\text{-}\kappa^3P)]PF_6$ (**7**) and the known Rh^I monohydride $[RhH(DMFU\text{-}\kappa^2C^{2,3})(triphos\text{-}\kappa^3P)]$ (**8**) (DMFU = dimethyl fumarate (dimethyl but-2-enedioate)) [22b,c], were also formed in comparable amounts.

With time, the concentration of the bis-Q complexes increased at the expense of that of **7** and became largely predominant only after the NMR tube was heated at 40° for 15 min (*Fig. 1,c*). In the meantime, the resonance due to **8** disappeared, and the hydride-containing Rh complex **5** began to form [$^{31}P\{^1H\}$-NMR: δ 27.1 (*m*, P_A); 25.2 (*m*, P_M); 9.1 (*m*, P_Q). ^{1}H-NMR: δ −8.55 (*dm*, *J*(H,P) = 153, Rh–H)]. A parallel ^{1}H-NMR

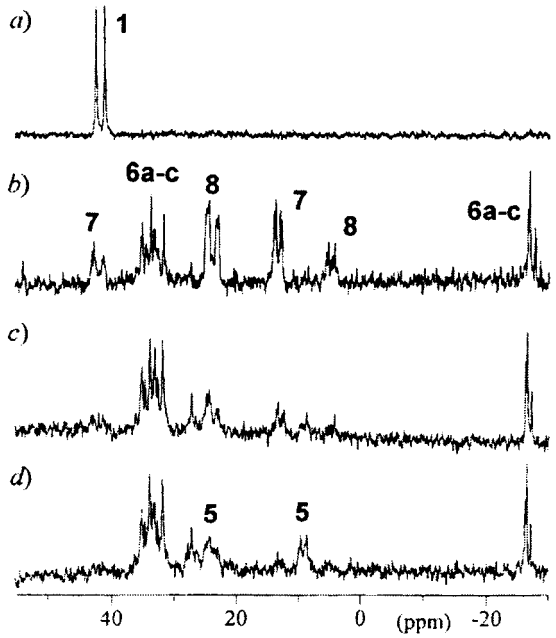

Fig. 1. *$^{31}P\{^1H\}$-HP-NMR Study* (sapphire tube, (D_8)THF, 81.01 MHz) *of the catalytic hydrogenation of Q* (220 mM) *in the presence of* **1**, (Q/**1** 40 : 1). *a*) At r.t. and ambient pressure *b)* pressurized to 30 bar with H_2 at r.t., *c*) after heating to 40° for 15 min, and *d*) after heating to 40° for 120 min.

Scheme 4

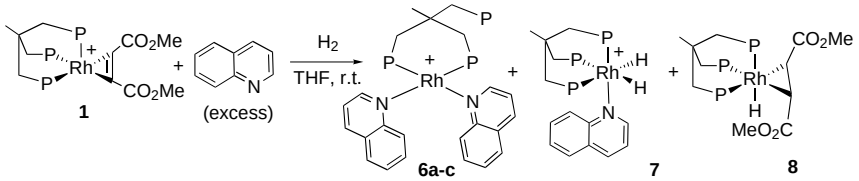

investigation showed that the selective reduction of Q to THQ occurred only after heating to 40°. After 2 h heating at 40°, *ca.* 40% of the initial Q was reduced to THQ, and $^{31}P\{^1H\}$-NMR spectroscopy showed the presence of **6a – c** (eventually accompanied by minor amounts of **6x – z**) and of **5** (*Fig. 1, d*). The latter product was obtained also by hydrogenation of **8** in THF in the absence of Q, and, like **8**, proved to be inactive for the hydrogenation of Q (*vide infra*). For this reason, the elucidation of its structure was not considered a primary objective. Moreover, its formation under real autoclave conditions was negligible.

The reactions illustrated in *Scheme 4* are not difficult to rationalize as **1** is a precursor to the fragment $[Rh(H)_2(triphos)]^+$ (*Scheme 3*), which may actually fix either one or two (*via* H_2 elimination [21]) molecules of Q to yield **7** and **6a – c**, respectively. Even the formation of the fumarate-hydride complex **8** is rather straightforward as it is known that hydrogenation of **1** in THF is a stepwise process involving the intermediacy of the fumarate complex $[Rh(DMFU\text{-}\kappa^2C^{2,3})(triphos)]^+$

[22a][23a]. The presence of a terminal hydride in **8** is reasonably due to the occurrence of heterolytic splitting of H_2 in the basic environment of the reaction mixture containing a large excess of Q. For d^6 metal complexes with triphos the occurrence of H_2 heterolytic splitting in basic media is a routine reaction, indeed [20c][21b,d,e]. In the case at hand, a recent paper has shown that the hydrogenation of **1** in THF gives the trihydride $[Rh(H)_3(triphos)]$ (**9**) in the presence of a base [21e].

In an attempt to mimick analogous autoclave reactions (see below), the hydrogenation of **1** was studied by HP-NMR spectroscopy at lower concentrations of Q.

With an initial 70 mM concentration of Q, the following observations were made: *i*) The dihydride complex **7** was the first and largely prevalent Rh product formed at room temperature. *ii*) Appreciable formation of the bis-Q complexes occurred only when the tube was heated to 40°. *iii*) The reduction of Q started already at room temperature and was complete after 1 h at 40°. *iv*) The binuclear complex **5** became the predominant Rh product when all Q had been converted to THQ.

When the concentration of Q was reduced further to 30 mM, the conversion of Q to THQ occurred already at room temperature and was much faster in comparison to the reaction with 70 mM Q. No formation of the bis-Q derivatives was detected by NMR at any stage of the conversion of Q to THQ, which required only 30 min to be complete at room temperature. Under these conditions, **5** and **7** were the predominant products, while the formation of **8** was rather marginal.

In summary, the HP-NMR studies have shown that the hydrogenation rate of Q has an inverse concentration dependence in the presence of **1**. The two major products visible on the NMR time scale in catalytic conditions contain Q-κN ligands. The catalytically inactive Rh^I compound **8** is formed in an appreciable amount only when the hydrogenation of Q does not occur or is very slow. Above 40°, **8** apparently degrades to **5**. In no case was either 1,2-dihydroquinoline (1,2-DHQ) or 1,4-dihydroquinoline (1,4-DHQ) detected as an intermediate in the reduction of Q to THQ.

The hydrogenation of the 2-vinylthiophenolate complex **2** in the presence of Q has been similarly studied by HP-NMR spectroscopy. However, no useful information was obtained: in particular, neither reduction of Q nor formation of a Q complex was observed, and the starting Rh complex underwent degradation to several compounds as occurs in THF [21a,f,g].

2.1.3. *Hydrogenation of the Catalyst Precursors in THF in the Presence of Triflic Acid.* Since the rate of hydrogenation of Q has been found to increase remarkably in the presence of a *Brønsted* acid (see below), the hydrogenation of the Rh precursor **1** was studied by HP-NMR spectroscopy in (D_8)THF containing CF_3SO_3H (TfOH).

A selection of $^{31}P\{^1H\}$-HP-NMR spectra is reported in *Fig. 2*.

The precursor **1** was stable in the presence of 3 equiv. of TfOH under N_2 (*Fig. 2, a*), whereas it reacted already at room temperature when the tube was pressurized with 30 bar H_2 (*Fig. 2, b*). After 1 h at 40°, all of **1** had disappeared (*Fig. 2, c*). Formed in its place was a mixture of two fluxional products featured by broad $^{31}P\{^1H\}$-NMR resonances centered at 42 and -13 ppm as well as a doublet of quartets at -6.29 ppm in the ^{1}H-NMR spectrum ($J(HRh) = J(HP)_{cis} = 7.5$ Hz; $J(HP)_{trans} = 202.6$ Hz). The temperature of the probe-head was then decreased to 20, 0, and -30°. The

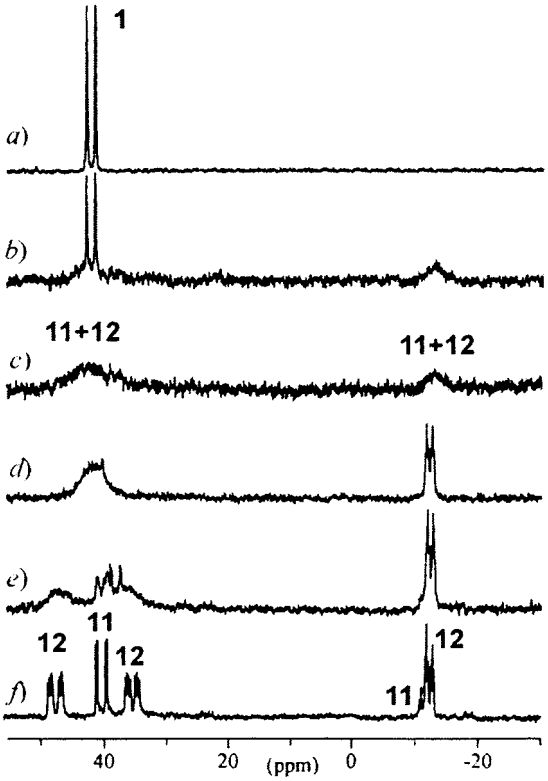

Fig. 2. *$^{31}P\{^1H\}$-HP-NMR Study* (sapphire tube, (D_8)THF, 81.01 MHz) *of the hydrogenation of* **1** *in the presence of TfOH* (TfOH/**1** 3:1). *a*) At r.t. and ambient pressure, *b*) under 30 bar H_2 for 20 min at r.t., *c*) after heating 60 min at 40°, *d*) after cooling to r.t., *e*) to 0°, and *f*) to −30°.

corresponding $^{31}P\{^1H\}$-NMR spectra are shown in *Fig. 2, d, e*, and *f*, respectively. At −30°, the dynamic process affecting the triphos-containing species was completely frozen out, and two Rh complexes in a 1:2 ratio (**11** and **12**) were clearly visible, which have been unequivocally identified through their independent synthesis as outlined in *Scheme 5*.

Scheme 5

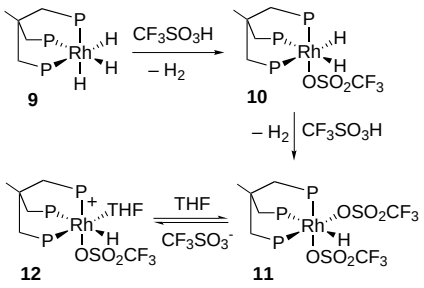

The products that were actually formed by hydrogenation of **1** in THF in the presence of a threefold excess of TfOH are $[RhH(OSO_2CF_3)_2(triphos)]$ (**11**) and $[RhH(OSO_2CF_3)(THF)(triphos)]$ (**12**). The dihydride derivative $[Rh(H)_2(O\text{-}SO_2CF_3)(triphos)]$ (**10**) was intercepted in the stoichiometric protonation of the trihydride **9** used in the independent synthesis of **11** and **12**. These two complexes are in rapid equilibrium in room temperature THF solution (*Scheme 5*). The bis-triflate complex **11** was isolated as pale yellow microcrystals by reacting **9** with three equivalents of TFOH in THF, followed by addition of heptane. The spectroscopic characterization of the new compounds **10**, **11**, and **12** was straightforwardly obtained by routine NMR methods. In the slow-exchange regime (*Fig. 2, f*), **11** and **12** exhibit canonical $^{31}P\{^1H\}$-NMR AM_2X and AMQX patterns, respectively, with hydride resonances at -6.23 ppm for **11** (dq, $J(H,P_{trans}) = 196.2$, $J(H,P_{cis}) = J(H,Rh) = 7.8$ Hz) and at -6.15 ppm for **12** (dq, $J(H,P_{trans}) = 195.3$, $J(H,P_{cis}) = J(H,Rh) = 7.4$ Hz).

The substitution of TsOH for triflic acid in the reaction with the trihydride **9** yielded $[RhH\{OSO_2(C_6H_4)p\text{-}Me\}_2(triphos)]$ analogous to **11**, while the use of $HBF_4 \cdot OEt_2$ led exclusively to the formation of the binuclear tetrahydride **4**.

Interestingly, the addition of Q to a (D_8)THF solution of **11** resulted in the complete transformation of the starting Rh complex into **6a–c** (*Scheme 6*). Consistent with the results reported in *Scheme 6*, the hydrogenation of **1** in a (D_8)THF solution containing also 40 equiv. of Q and 10 equiv. of CF_3SO_3H gave selectively **6a–c**, eventually contaminated by the oxidation product **6x–z** (HPNMR and autoclave experiments). Half of the Q was selectively converted to THQ in *ca.* 60 min at 40° (*Fig. 3*). In the presence of an excess of strong protic acids like TfOH or TsOH, the hydrogenation of **2** with or without added Q, gave identical results to analogous hydrogenation reactions of **1**, which is consistent with the similar catalytic activity exhibited by the two precursors (see below).

Scheme 6

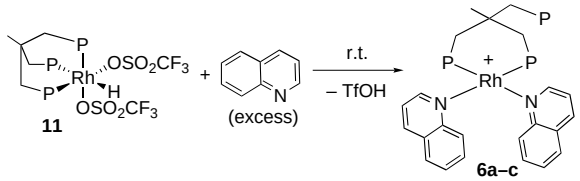

2.2. *Synthesis and Characterization of the Mono-Q and Bis-Q Complexes* **7** *and* **6a–c/6x–z**. While the authentication of **7** was readily accomplished by comparing its spectroscopic properties with those of a pure sample independently prepared by treatment of a THF solution of $[RhCl(H)_2(triphos)]$ [22a] with $TlPF_6$ in the presence of Q, the characterization of **6a–c**, particularly when contaminated by its phosphine oxide derivatives **6x–z**, required a long and accurate NMR analysis. Details of this study are given below as they represent a paradigmatic case of the potential of multidimensional NMR spectroscopy for the elucidation of complicated structures and/or mixtures of products in solution.

Besides *in situ* HP-NMR and batch catalytic experiments, the mixture of geometrical isomers denoted as **6a–c** was also synthesized by independent methods

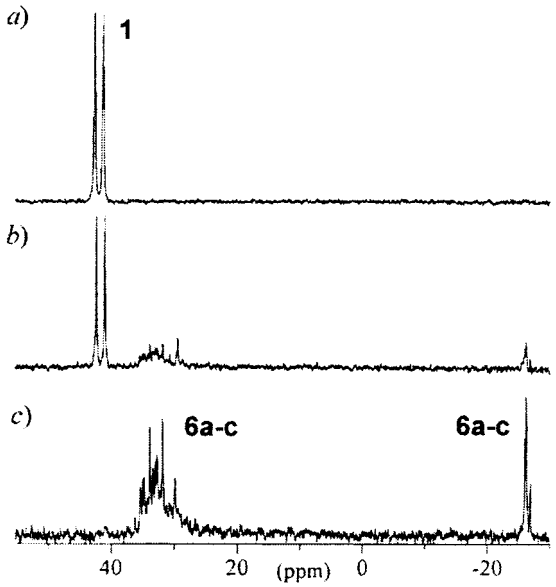

Fig. 3. *$^{31}P\{^1H\}$-HP-NMR Study* (sapphire tube, (D_8)THF, 81.01 MHz) *of the catalytic hydrogenation of Q in the presence of* **1** *and TfOH* (Q/TfOH/**1** 40 : 10 : 1). *a*) at r.t. and ambient pressure, *b*) pressurized to 30 bar with H_2 for 15 min at r.t., and *c*) after heating to 40° for 60 min.

involving the plain displacement of ligands from appropriate Rh^I-triphos precursors. Two of these methods are reported in *Scheme 7* and described in the *Exper. Part*. Slow transformation of **6a**–**c** into **6x**–**z** was observed when a controlled amount of air was allowed to react with a solution of **6a**–**c** contained in either a NMR tube or an autoclave. In no case, however, was it possible to isolate either **6a**–**c** or **6x**–**z** in the solid state, an excess of Q being necessary for their stabilization.

Scheme 7

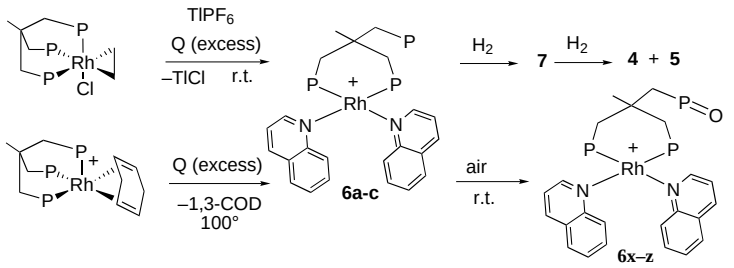

Consistent with the HP-NMR studies, the hydrogenation (30 bar H_2) of a (D_8)THF solution of **6a**–**c**/**6x**–**z** obtained by either method shown in *Scheme 7*, gave the dihydride **7**, and then a mixture of **4** and **5** when all Q was consumed.

A high-resolution ^1H- and $^{31}P\{^1H\}$-NMR study has been performed on a (D_8)THF solution of **6a**–**c**/**6x**–**z** prepared *in situ* by reaction of **11** with excess Q.

The 1D $^{31}P\{^1H\}$- and 2D $^{31}P\{^1H\}$-COSY NMR spectra show the sample to contain a mixture of six Rh compounds denoted as **6a**–**c**, and **6x**–**z**. A small amount of free triphos oxide was also detected. The molar ratio of the six complexes in the sample studied was **6a**/**6b**/**6c**/**6x**/**6y**/**6z** ≅ 6 : 4 : 2 : 3 : 2 : 1[1]). After the solution was exposed to air, the isomeric product ratio within each series **6a**–**b** or **6x**–**z** did not vary, but the overall concentration of **6x**–**z** increased at the expense of **6a**–**c**. $^{31}P\{^1H\}$-NMR Data for all compounds are reported in *Table 1*.

Table 1. *$^{31}P\{^1H\}$-NMR Data of Complexes* **6** [a])

Compound	**6a**	**6b**	**6c**	**6x**	**6y**	**6z**
Chemical shifts	$P_{A1} = 34.93$ $P_{A2} = 33.98$ $P_{A3} = -26.28$	P_{B1} (2 P) = 32.80 $P_{B2} = -26.01$	P_{C1} (2 P) = 34.06 $P_{C2} = -27.19$	$P_{X1} = 33.80$ $P_{X2} = 31.91$ $P_{X3} = 28.00$	P_{Y1} (2 P) = 31.71 $P_{Y2} = 27.93$	P_{Z1} (2 P) = 33.42 $P_{Z2} = 26.59$
Coupling constants	$^2J_{P_{A1},P_{A2}} = 65$ $^4J_{P_{A1},P_{A3}} = {}^4J_{P_{A2},P_{A3}} = 3.5$ $^1J_{P_{A1},Rh} = 163$	$^4J_{P_{B1},P_{B2}} = 3.0$ $^1J_{P_{B1},Rh} = 163$	$^4J_{P_{C1},P_{C2}} = 2.0$ $^1J_{P_{C1},Rh} = 162$	$^2J_{P_{X1},P_{X2}} = 64$ $^4J_{P_{X1},P_{X3}} = {}^4J_{P_{X2},P_{X3}} = 3.5$ $^1J_{P_{X1},Rh} = 162$	$^4J_{P_{Y1},P_{Y2}} = 3.0$ $^1J_{P_{Y1},Rh} = 162$	$^4J_{P_{Z1},P_{Z2}} = 2.0$ $^1J_{P_{Z1},Rh} = 162$

[a]) 161.98 MHz, (D_8)THF, 294 K. Chemical shifts in ppm, coupling constants in Hz.

The six Rh complexes have been identified and their ^{1}H-NMR characteristics unequivocally assigned by a combination of 1D and 2D NMR techniques (see *Exper. Part*). Selected ^{1}H-NMR data are reported in *Table 2*. The compounds constitute a family of geometric isomers (*syn-syn*, *anti-anti*, *syn-anti*) having square-planar geometry and the general formula [*cis*-MeC(CH_2P(J)Ph_2)(CH_2PPh_2-κP)$_2$Rh(Q-κN)$_2$]$^+$, where J represents a pair of electrons for **6a**–**c** and an O-atom for **6x**–**z** (*Fig. 4*). The dissociation of a phosphane arm of triphos in Rh^I complexes (arm-off mechanism) with formation of square-planar compounds has several precedents in either catalytic intermediates (*e.g.*, in the hydroformylation of olefins catalyzed by [RhH(CO)(triphos)] [22a]) or stable species (*e.g.*, [Rh(triphos-κ^2P)(η^6-$C_6H_5BPh_3$)] [26]).

In all compounds **6a**–**c** and **6x**–**z**, the Q molecules have a N–metal bond as shown by the chemical-shift difference of corresponding proton resonances in coordinated and free Q[2]), and by the coupling of the H–C(2) protons to the P-atoms in the *trans* position with respect to the corresponding Q ligand (*Table 1*). Sections of the ^{1}H-TOCSY and ^{1}H-^{31}P correlation spectra are reported in *Fig. 5*. No NMR resonance attributable to protons of either THQ or π-Q was detected.

In each complex, two P-atoms are bonded to the metal (^1J(P,Rh) *ca.* 163 Hz) in *cis* fashion with a ^2J(P,P) coupling constant of *ca.* 64 Hz [27][28]. The third P-atom is not

---

1) Calculated from $^{31}P\{^1H\}$- and ^{1}H-NMR integration.

2) As compared to the corresponding resonances in free Q, the signals of the H–C(2), H–C(3), and H–C(5) nuclei in π-coordinated Q show a downfield shift, whereas the H–C(5), H–C(6), H–C(7), and H–C(8) protons show an upfield shift. In N-coordinated Q, all the ring protons show a downfield shift. Typical values for H–C(2) and H–C(8) are *ca.* +0.5 and +0.7 ppm, resp. [7b]. In **6a**–**c**/**6x**–**z**, a univocal trend of the chemical-shift variation of the H-atoms in coordinated and free Q is not easily distinguishable, likely due to *chemical shielding* effects. However, a diagnostic downfield shift can be given for of the H–C(8) protons (+1.9 – +0.9 ppm).

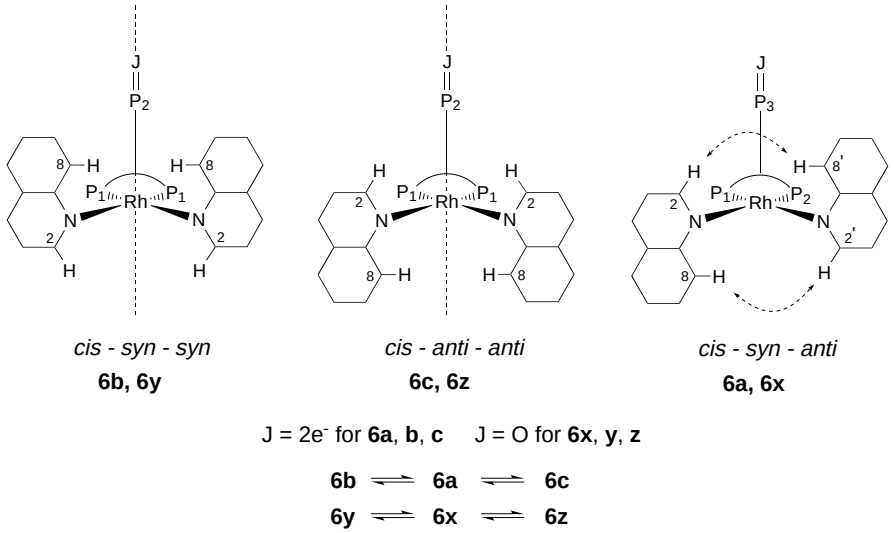

Fig. 4. *Schematic view of the bis-Q complexes* **6a**–**c**, **6x**–**z** *in the coordination plane of the metal.* The dashed lines represent the symmetry planes, while the dashed arrows represent the significant NOEs.

Table 2. *Selected* ^{1}*H-NMR Chemical Shifts* [ppm] *and Coupling Constants* [Hz] *of Complexes* **6**[a])

	Compound							
Nucleus	**6a**		**6b**	**6c**	**6x**		**6y**	**6z**
H–C(2)	9.48 (*dt*) [b])	8.89 (*dt*) [c])	10.18 (*d*, 2 H) [b])	9.73 (*d*, 2 H) [b])	9.54 (*dt*) [b])	8.70 (*dt*) [c])	10.19 (*d*, 2 H) [b])	9.57 (*d*, 2 H) [b])
	J(H,H) = 5.0	*J*(H,H) = 5.0	*J*(H,H) = 6.0	*J*(H,H) = 5.0	*J*(H,H) = 5.0	*J*(H,H) = 5.0	*J*(H,H) = 6.0	*J*(H,H) = 5.0
	J (H–P) = 2.5	*J*(H,P) = 2.5			*J*(H,P) = 2.5	*J*(H,P) = 2.5		
H–C(4)	7.75 [d])	7.71 [d])	7.80 [d]) (2 H)	7.77 [d]) (2 H)	7.72 [d])	7.68 [d])	7.78 [d]) (2 H)	7.75 [d]) (2 H)
H–C(6)	7.01 [d])	6.66 [d])	7.33 [d]) (2 H)	7.10 [d]) (2 H)	7.03 [d])	6.55 [d])	7.32 [d]) (2 H)	7.01 [d]) (2 H)
H–C(8)	9.64 (*d*) [e])	9.90 (*d*)	9.02 (*d*, 2 H)	9.34 (*d*, 2 H)	9.64 (*d*) [e])	9.97 (*d*)	9.04 (*d*, 2 H)	9.40 (*d*, 2 H)
	J(H,H) = 8.5	*J*(H,H) = 8.5	*J*(H,H) = 8.0	*J*(H,H) = 8.0	*J*(H,H) = 8.5	*J*(H,H) = 8.5	*J*(H,H) = 8.0	*J*(H,H) = 8.5
H–C(7)	7.84 [d])	8.08 [d])	7.30 [d]) (2 H)	7.52 [d]) (2 H)	7.81 [d])	8.12 [d])	7.29 [d])[e]) (2 H)	7.59 [d]) (2 H)
H–C(5)	7.32 [d])	7.48 [d])	7.25 [d]) (2 H)	7.38 [d]) (2 H)	7.36 [d])	7.50 [d])	7.29 [d])[e]) (2 H)	7.40 [d]) (2 H)
H–C(6)	7.26 [d])	7.36 [d])	7.04 [d]) (2 H)	7.14 [d]) (2 H)	7.24 [d])	7.38 [d])	7.07 [d]) (2 H)	7.20 [d]) (2 H)

[a]) 500.132 MHz, (D_8)THF, 294 K. [b]) A coupling to P_1 is apparent in the ^{1}H-^{31}P correlation. [c]) A coupling to P_2 is apparent in the ^{1}H-^{31}P correlation. [d]) Partially masked by other proton resonances. Detected from the ^{1}H-TOCSY spectrum. [e]) Overlapped resonances.

coordinated in **6a**–**c** (δ −26.0/−27.2) and oxidized to phosphine oxide in **6x**–**z** (δ 26.6/28.0). In complexes **6b**, **6c**, **6y**, and **6z**, the two coordinated arms of triphos and the two Q ligands appear to be chemically equivalent in the ^{31}P{^{1}H}- and ^{1}H-NMR spectra, which indicates that, in THF solution at 21°, these complexes adopt a time-averaged preferred conformation in which a symmetry plane perpendicular to the coordination plane of the metal bisects the P(1)–P(1) and N–N axes. This arrangement and the σ plane are schematically represented in *Fig. 4*. In contrast, 1D-NMR spectra show no symmetry elements for the complexes **6a** and **6x**. Accordingly, the *syn-anti* structure can unequivocally be assigned to **6a** and **6x** and, thus, each complex exists as a couple of

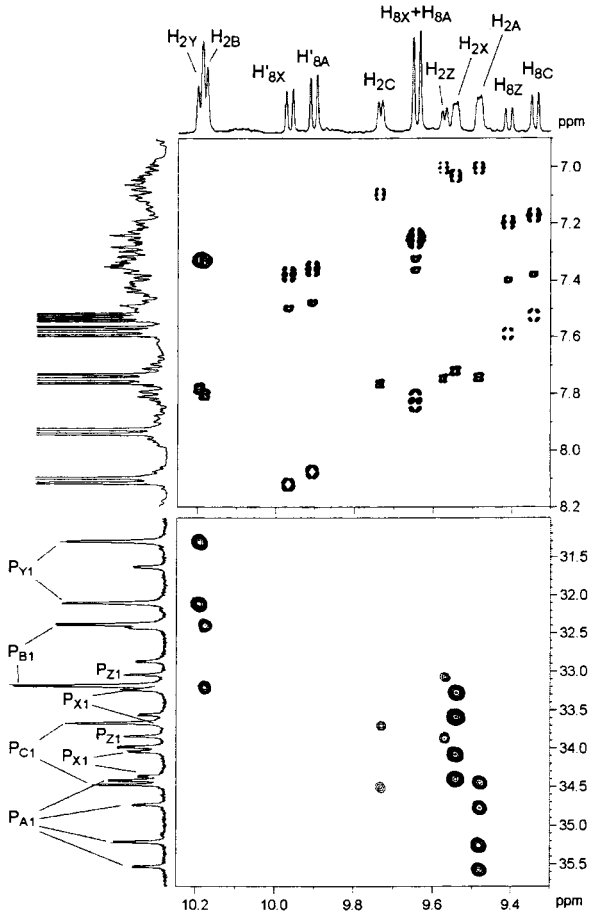

Fig. 5. *Section of the* ^{1}*H-TOCSY spectrum* (upper) *and 2D* ^{1}*H-*^{31}*P correlation* (lower) *of the* **6a–c/6x–z** *mixture* (500.13 MHz, (D_8)THF, 21°)

atropisomers. The two diastereotopic Q ligands in **6a** and **6x** show strong NOE interactions between the H–C(2) and H–C(8) protons belonging to different Q molecules (*Fig. 4*). A representative section of the ^{1}H-NOESY spectrum of **6a–c/6x–z** is reported in *Fig. 6*.

A *skew* conformation for the six-membered triphos-Rh chelate rings in these complexes is ruled out by the presence of the reflection plane, whilst *boat* or *chair* conformations are equally plausible [29][30]. Accordingly, irrespective of the conformation, the phenylphosphino rings give rise to two couples of *pseudo*-equatorial and *pseudo*-axial groups with respect to the coordination plane of Rh. The arrangement of the phenylphosphino groups is shown below.

The *ortho*-protons of each phenylphosphino group have been assigned on the basis of the 2D ^{1}H-^{31}P-NMR correlations. The *ortho* protons of the *pseudo*-equatorial Ph moieties are distinguished from the *pseudo*-axial *ortho* Ph protons by their higher-field

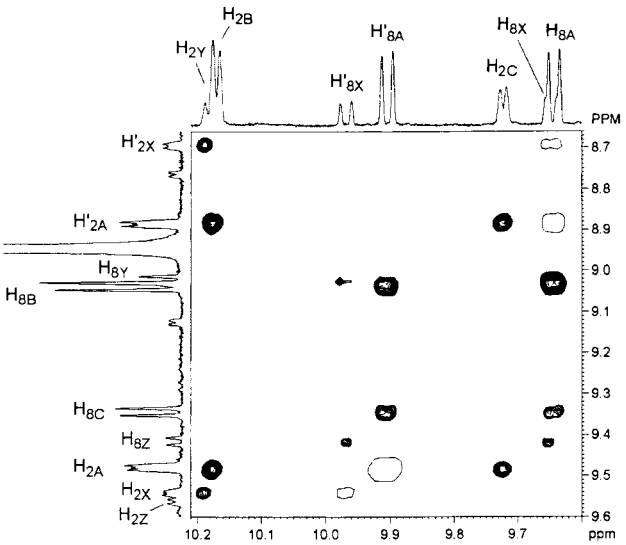

Fig. 6. *Section of the ^{1}H-NOESY spectrum of the* **6a**–**c**/**6x**–**z** *mixture* (500.13 MHz, (D_8)THF, 21°, τ_m 0.65 s). Positive-phased (exchange) cross-peaks are represented by filled circles; negative phased (NOE) cross-peaks are represented by open circles.

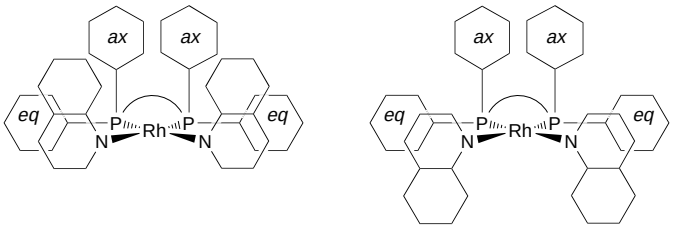

chemical shifts[3]). ^{1}H-NOESY and ^{1}H-ROESY spectra of the *syn-syn* isomers show strong NOE interactions between the *ortho* protons of the axial Ph groups and the H–C(8) protons of Q, which confirms that these protons lie on the same side of the coordination plane of Rh (the adopted nomenclature refers to this arrangement). This kind of interaction has not been seen for the H–C(2) protons. The situation is just opposite for the *anti-anti* isomers, so that one can easily identify **6b** and **6y** as the *anti-anti* isomers, and **6c** and **6z** as the *syn-syn* isomers. Following this reasoning, the H–C(8′) and H–C(2′) protons (*Figs. 4* and *5*) may be identified as those belonging to the *syn* Q ligand in **6a** and **6x**.

---

[3]) This assignment has been made on the basis of the stronger *shielding effect* exerted by the Q ligands on the *pseudo*-equatorial phenyls in comparison to the *pseudo*-axial Ph protons, as they lie 'out' of the coordination plane of the metal. Similar behavior has been reported for comparable complexes, see, *e.g.*, [30–33]. The ^{1}H-NMR chemical shifts of the *σ*-phenylphoshino protons in **6a**–**c**/**6x**–**z** are available upon request from the authors.

The geometric isomerism in these square-planar bis-Q complexes is apparently due to hindered rotation of the Q ligands about the Rh–N axis because of their mutual interaction and the presence of the phenylphosphino ligands. The **6a**–**c** isomers (as well as **6x**–**z**) exhibit a slow-exchange-motion regime, as demonstrated by the ^{1}H-ROESY and ^{1}H-NOESY spectra (*Fig. 6*) [34][35]. Consistent with the interconversion of the isomers, the proton-exchange pattern observed for the **6a, 6b**, and **6c** isomers can be illustrated as in *Scheme 8* (obviously, a similar pattern can be proposed for **6x**–**z**).

Scheme 8

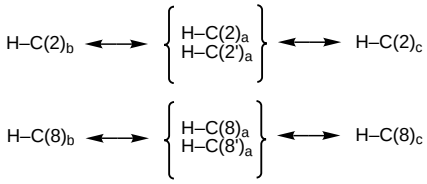

No direct-exchange peak relating the Q protons of **6b** to those of **6c** (nor those of **6y** to those of **6z**) was observed. This means that the conversion of one isomer to the other takes place exclusively upon rotation of only one Q ligand at a time, *i.e.*, no simultaneous rotation of the two coordinated Qs about the Rh–N bonds occurs.

The observed concentrations of the various isomers in solution (*syn-anti* > *anti-anti* > *syn-syn*) can be rationalized in terms of their relative stabilities. The intramolecular steric strain that differentiates the three isomers is occasioned by two types of repulsive interactions involving either the axial phenyls and the *syn* quinoline ligands or the two coordinated quinolines. In this picture, the *syn-syn* isomers are the least stable, as they can undergo both interactions. In the *anti-anti* isomers, the repulsion with the axial Ph groups is minimized, but the Q–Q interactions are still present. The latter interactions are evidently the most destabilizing ones as the isomer concentration decreases in the order *syn-anti* > *anti-anti*.

2.3. *Catalytic Hydrogenation of Q.* Complex **1** is an efficient and selective homogeneous catalyst for the hydrogenation of Q to THQ. As shown in *Table 3*, a turn-over frequency (TOF) of 98 (mol product (mol cat × h)$^{-1}$) was obtained already at 60° (*Entry 2*), while at 40°, the TOF decreased to 43 (*Entry 1*). Substitution of **7** for **1** gave a much higher conversion at 40° (*Entry 3*) and a comparable result at 60° (*Entry 4*). To produce high conversion even at 40° with **1**, some triflic acid was added to the mixture (*Entry 5*). However, the addition of too much acid, as in *Entries 6* and *7*, was found to inhibit the hydrogenation activity due to two possible negative effects: *i*) excess triflate anions can compete with Q for coordination to Rh (thus disfavoring the conversion of **10** to **7**), and *ii*) Q can be protonated at the N-atom to give QH^+ that, as shown in *Entry 8*, is not easily hydrogenated. In actuality, QH^+ has no way of binding the metal center through the N-atom, which is crucial for hydrogenation [3], and the small activity observed is apparently due to the equilibrium concentration of nonprotonated Q. The beneficial effect of the acid on the catalytic activity of **1** at 40° is ascribed to the conversion of inactive Rh^I by-products that may form in the catalytic mixture. As a matter of fact, the presence of an excess of TfOH makes the Rh^I

Table 3. *Hydrogenation of Q to THQ Catalyzed by Rhodium-triphos Complexes* [a])

Entry	Catalyst	TfOH [equiv.]	*T* [°]	Conversion [%]
1	**1**	0	40	43
2	**1**	0	60	98
3	**7**	0	40	94
4	**7**	0	60	98
5	**1**	5–20	40	98
6	**1**	40	40	83
7	**1**	100	40	30
8	**1**	100 $QH^+(OTf)$ [b])	40	28
9	**2**	0	60	< 1
10	**2**	5	60	77
11	**2**	20	60	98
12	**8**	0	60	0
13	**8**	20	60	95

[a]) Experimental conditions: [Cat] 0.022 mmol, Q/Cat ratio 100 : 1, THF 30 ml, pH_2 30 bar, 1 h. [b]) Quinolinium triflate.

precursors **2** and **8** as efficient as **1** in the hydrogenation of Q (*Entries 9–13*).

NMR Analysis of the reaction mixtures collected at the end of selected catalytic runs showed the formation of the bis-Q adducts **6a–c**, while the presence of **5** was, in all cases, almost negligible. Occasionally, the formation of the phosphine oxide **6x–z** was also observed. However, when air was purposefully introduced into the autoclave prior to heating, the catalytic activity was almost totally inhibited.

2.4. *Kinetics Studies of the Hydrogenation of Q in the Absence of Acid.* To determine the dependence of the hydrogenation rate on the concentrations of Rh, H_2, and Q, a series of reactions were carried out with different initial concentrations of catalyst and reagents. The reactor contents were analyzed by GC every 10 min at constant temperature (60°) and internal pressure (*Table 4*). The H_2 concentrations in the liquid phase have been calculated on the basis of solubility data reported in the literature [36].

Table 4. *Kinetic Data for the Hydrogenation of Q with* **1** *as the Catalyst Precursor* [a])

$[Rh] \cdot 10^4$ [M]	pH_2 (psi)	$[H_2] \cdot 10^2$ [M]	$[Q] \cdot 10^2$ [M]	$k \cdot 10^3$ (min^{-1})
7.33	115	2.99	1.83	15.47
7.33	115	2.99	3.67	7.71
7.33	115	2.99	5.50	5.89
7.33	115	2.99	7.33	3.92
7.33	115	2.99	9.17	2.84
7.33	58	1.39	7.33	1.92
7.33	230	6.10	7.33	9.11
7.33	460	12.83	7.33	19.21
3.67	115	2.99	7.33	1.89
5.50	115	2.99	7.33	2.96
11.00	115	2.99	7.33	6.14

[a]) Experimental conditions: 30 ml THF, 60°, 1 h.

A simple rate equation that accounts for the hydrogenation of Q with the catalyst precursor **1** is:

$$-d[Q]/dt = d[THQ]/dt = k[Rh]^m[Q]^n[H_2]^p \quad (3)$$

Assuming that the Rh and H_2 concentrations do not vary over the time of each reaction (this is correct for experiments in which the amount of dissolved H_2 is much larger than that consumed in the reduction of the substrate), the above equation can be simplified as follows:

$$-d[Q]/dt = k[Q]^n \quad \text{with} \quad k = k[Rh]^m[H_2]^p \quad (4)$$

In an attempt to determine the dependence of the hydrogenation rate on [Q], the observed variations of [Q] *vs.* time in each experiment were plotted according to models of second-order $(1/[Q] - 1/[Q]_o)$, first-order $(\log([Q]_o/[Q]))$, or zero-order $([Q]_o/[Q])$ dependence. For all the experiments reported in *Table 4*, the plots $\log([Q]_o/[Q])$ *vs.* time gave straight lines with correlation coefficients as high as 99.9%. Accordingly, it was concluded that, in the range of $[Q]_o$ reported in *Table 4*, the reactions were first-order with respect to substrate concentration, and *k* was calculated for each experiment from the slope of the straight line obtained. As an example, *Fig. 7* shows a plot of $\log([Q]_o/[Q])$ *vs.* time for the reaction performed with the following parameters: $[Rh] = 7.3 \cdot 10^{-4}$ M, $[H_2] = 2.99 \cdot 10^{-2}$ M, and $[Q]_o = 7.3 \cdot 10^{-2}$ M. The first-order dependence on [Q] was maintained within the time investigated during which 42% of Q was converted to THQ. A treatment of the experimental data in terms of second-order dependence gave a better fit only for reactions carried out with $[Q]_o < 3 \cdot 10^{-2}$ M, while, for $[Q]_o > 7.3 \cdot 10^{-2}$ M, straight lines with correlation coefficients close to 100% were obtained when zero-order dependence on substrate concentration was assumed.

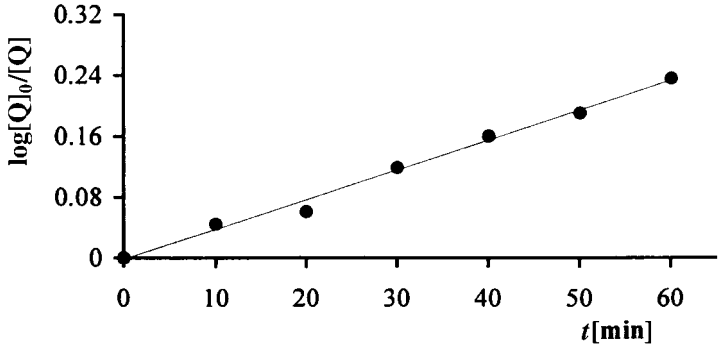

Fig. 7. *Plot of log ([Q]$_o$/[Q]) vs. reaction time for the hydrogenation of Q catalyzed by* **1** ($[Rh] = 7.3 \cdot 10^{-4}$ M, $[H_2] = 2.99 \cdot 10^{-2}$ M, $[Q]_o = 7.3 \cdot 10^{-2}$ M, 60°)

When, however, *k* was calculated for a series of reactions carried out with different $[Q]_o$ it was found that the values, instead of being equivalent within the experimental error, decreased exponentially with increasing $[Q]_o$. The observed dependence of *k* on

$[Q]_o$ clearly indicates that the hydrogenation of Q with **1** is a reaction whose rate law changes with the initial concentration of the substrate, in particular the rate decreases as $[Q]_o$ increases, which is consistent with the HP-NMR experiments. A typical reaction of this type is the hydroformylation of olefins catalyzed by $[RhH(CO)(PPh_3)_3]$ [37].

Much simpler reaction orders have been determined for $[H_2]$ and [Rh]. Experiments carried out at H_2 pressures of 4, 8, 15, and 30 bar were unequivocally consistent with first-order dependence on $[H_2]$ (*Fig. 8*). Analogously, experiments with $[Rh]_o = 3.67 \cdot 10^{-4}$, $5.50 \cdot 10^{-4}$, $7.33 \cdot 10^{-4}$, and $1.10 \cdot 10^{-3}$ M showed first-order dependence on [Rh] (*Fig. 9*).

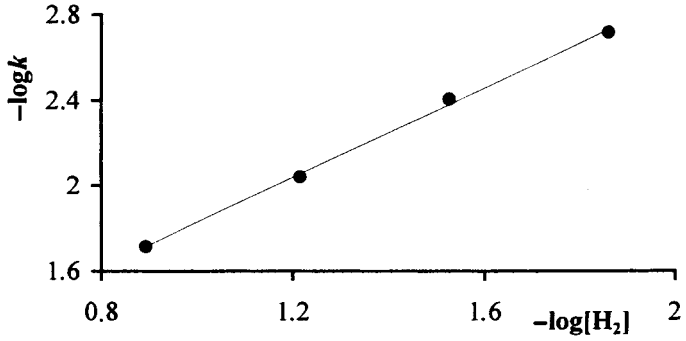

Fig. 8. *Dependence of the rate of hydrogenation of Q to THQ catalyzed by* **1** *on* $[H_2]$. Conditions are as in *Table 4*.

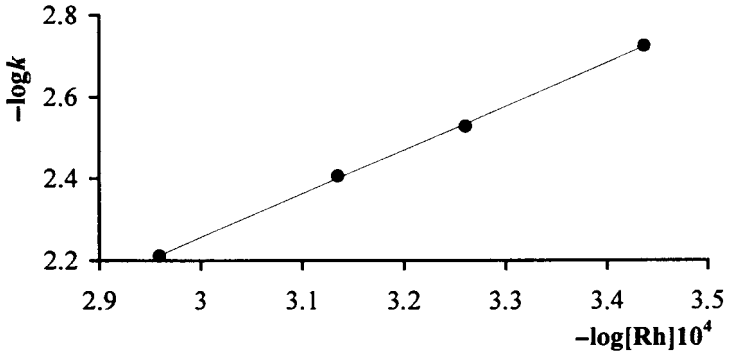

Fig. 9. *Dependence of the rate of hydrogenation of Q to THQ catalyzed by* **1** *on catalyst concentration.* Conditions are as in *Table 4*.

2.5. *Kinetic Studies of the Hydrogenation of Q in the Presence of Triflic Acid.* The dependences of the hydrogenation rate expressed as mmol THQ h^{-1} with respect to [Rh] and $[H_2]$ are reported in *Figs. 10* and *11*. The corresponding experimental data may be obtained as supplementary material from the authors.

While a first-order dependence can readily be assumed for both [Rh] and $[H_2]$, the rate dependence on [Q] and $[H^+]$ is very complicated due to the occurrence in the reaction mixtures of acid-base equilibria involving Q ($k_a = [Q][H^+]/[QH^+] = 10^{-4.9}$) and THQ ($k_a = [THQ][H^+]/[THQH^+] = 10^{-5}$). From *Figs. 12* and *13*, which show the

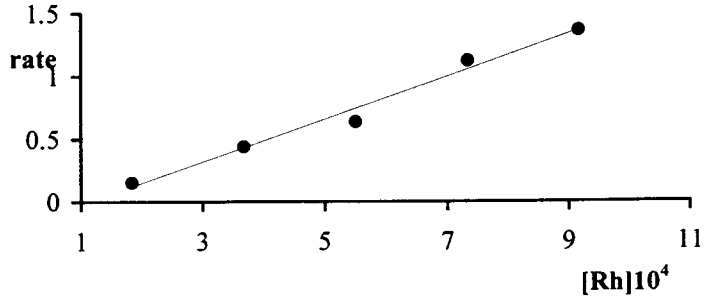

Fig. 10. *Dependence of the rate of hydrogenation of Q* ($7.33 \cdot 10^{-2}$ M) *to THQ catalyzed by* **1** *in the presence of TfOH* ($1.47 \cdot 10^{-2}$ M) *on catalyst concentration*

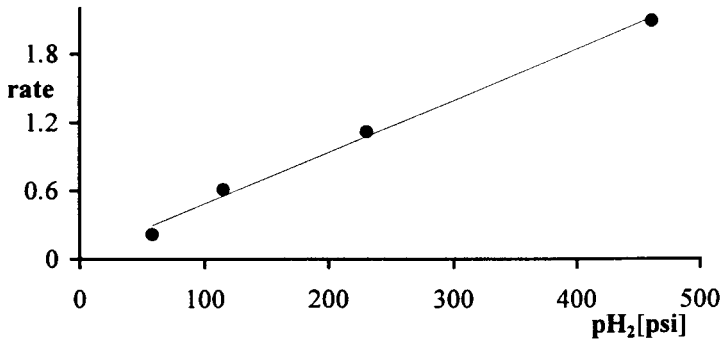

Fig. 11. *Dependence of the rate of hydrogenation of Q* ($7.33 \cdot 10^{-2}$ M) *to THQ catalyzed by* **1** ($7.33 \cdot 10^{-4}$ M) *in the presence of TfOH* ($1.47 \cdot 10^{-2}$ M) *on* H_2 *pressure*

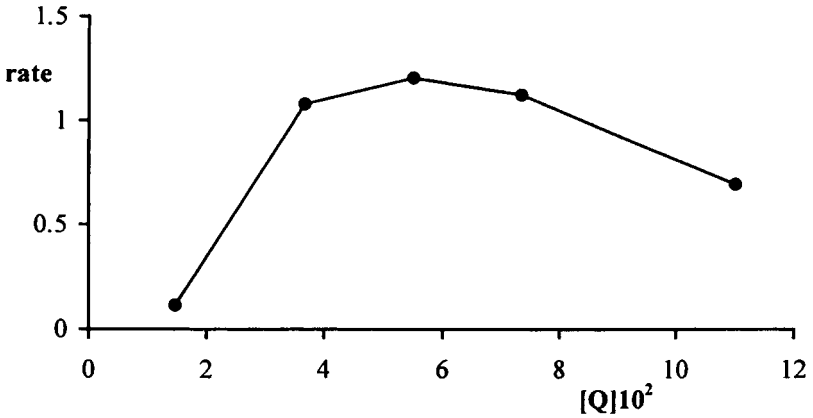

Fig. 12. *Dependence of the rate of hydrogenation of Q to THQ catalyzed by* **1** ($7.33 \cdot 10^{-4}$ M) *in the presence of TfOH* ($1.47 \cdot 10^{-2}$ M) *on substrate concentration*

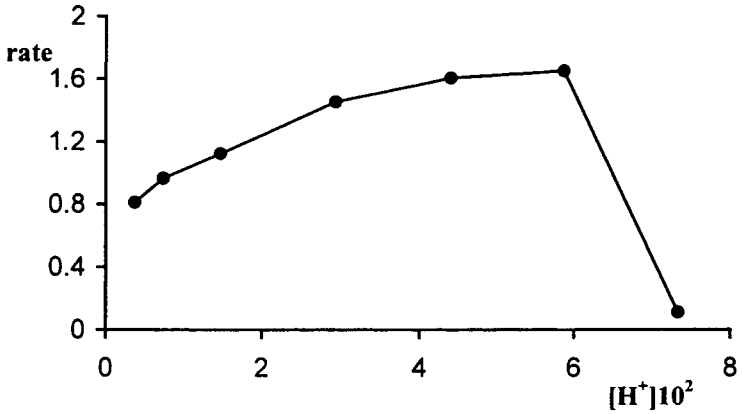

Fig. 13. *Dependence of the rate of hydrogenation of Q* ($7.33 \cdot 10^{-2}$ M) *to THQ catalyzed by* **1** ($7.33 \cdot 10^{-4}$ M) *in the presence of TfOH on* H^+ *concentration*

variation in rate as a function of [Q] and $[H^+]$, it may be concluded that low rates are expected when either $[H^+]$ or [Q] are low. For example, the rate at $[H^+]_{in} = 1.47 \cdot 10^{-2}$ M, increased by an order of magnitude by increasing [Q] from $1.47 \cdot 10^{-2}$ M to $3.67 \cdot 10^{-2}$ M, then the rate remained constant up to $[Q]_o = 8 \cdot 10^{-2}$ M. With a further increase in [Q], the rate decreased.

2.6. *Deuterium Gas Experiments.* Catalytic deuteration of Q was allowed to proceed to 40% conversion to THQ under D_2 (15 bar) in the presence of the catalyst precursor **1** at 60° (100 : 1 substrate to catalyst ratio). Analysis by GC/MS and ^{1}H-, ^{2}H-, and ^{13}C{^{1}H}-NMR of the reaction mixture showed that the formation of deuterated THQ was accompanied by that of D-enriched Q (*Scheme 11*). In particular, THQ was found to contain 1.1 D-isotope at position 2 and 1 D-isotope each at positions 3 and 4. The enrichment of deuterium at the 2-position in THQ is attributable to reversible H/D exchange mediated by the metal before D transfer (see *Scheme 9*). According to previous reports [7a,i,k], the observed line-width value of 15 Hz for the multiplets due to both H–C(3) and H–C(4), might indicate the occurrence of *cis*-deuteration. The N-atom was found to be nondeuterated as a result of rapid H/D exchange of the deuterium in this position due to the presence of protic impurities during workup [7a,i,k]. As regards the residual Q, 20% deuterium enrichment occurred at the 2-position as indicated by ^{1}H-NMR integration and confirmed by the GC/MS analysis showing a *m/z* 130 ion in *ca.* 20% relative abundance.

Scheme 9

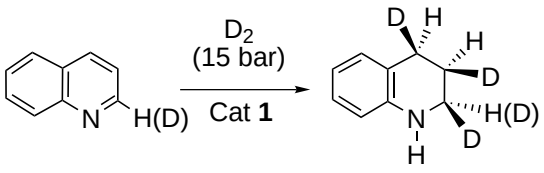

2.7. *Catalytic Hydrogenation of 1,2-Dihydroquinoline* (1,2-DHQ). To obtain further information on the mechanism of hydrogenation of Q by **1**, experiments of competitive reduction of Q and 1,2-DHQ (*Scheme 10*) have been carried out in sapphire HP-NMR tubes. Details of the procedure employed are provided in the *Exper. Part.*

Scheme 10

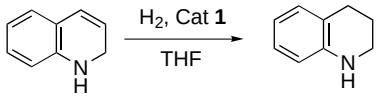

Under experimental conditions fully comparable to those used in the autoclave reactions ($[Rh] = 7.33 \cdot 10^{-4}$ M; $[Q]_o = 7.33 \cdot 10^{-1}$ M; $[1,2\text{-DHQ}]_o = 7.33 \cdot 10^{-1}$ M), it was found that 1,2-DHQ is hydrogenated to THQ *ca.* eight times faster than Q.

3. Discussion. - 3.1. *The Mechanism of Hydrogenation of Q to THQ Catalyzed by* **1**. In *Scheme 11* is reported the mechanism we propose for the selective hydrogenation of Q to THQ in the presence of **1** as univocally indicated by D_2 experiments, *in situ* HP-NMR spectra, kinetic studies, identification of catalytically relevant intermediates, and reactions with independent Rh compounds or partially reduced N-heterocycles. The proposed mechanism can be extended also to the reactions catalyzed by precursor **2** in the presence of a slight excess of protic acid, as the main role of the latter is exclusively to convert catalytically inactive [RhH(triphos)] to active $[Rh(H)_2(triphos)]^+$.

Prior to any catalytic step, the precursor **1** is hydrogenated to give dimethyl succinate and the $14e^-$ fragment $[Rh(triphos)]^+$. This electronically unsaturated system coordinates a Q molecule to attain the $16e^-$ configuration that enables Rh to bring about the oxidative addition of H_2 (*Steps a–b*). The Rh^{III} dihydride **7** has been actually intercepted under standard catalytic conditions (60°, $[Q] \leq 70$ mM). In the presence of a larger excess of Q, the coordination of a second Q molecule competes with H_2 oxidative addition and the bis-Q complexes **6a–c** may form (*Step c*). When this happens, the hydrogenation rate is slowed as the number of catalytically active Rh-atoms decreases.

Under the experimental conditions employed, **7** largely predominates over **6a–c**, and the hydrogenation of the C(2)=N bond of Q is fast. It has been amply demonstrated that a change in the Q bonding mode from κN to (1,2-η) is required to accomplish the conversion of Q to 1,2-DHQ (*Step d*) [3][7–9]. In principle, the hydrogenation of Q may also proceed through the intermediate 1,4-DHQ [9e]. In our case, this alternative reaction path has been ruled out by the lack of deuterium incorporation in the 4-position of the residual Q as well as the presence of one deuterium label only in the 4-position of THQ.

The reduction of the C(2)=N bond would occur by transfer of hydride from Rh to C(2), which, according to charge density studies [9c], is the most electrophilic site in Q (*Step e*). A reductive elimination step involving the residual hydride ligand and the amide N-atom ultimately generates 1,2-DHQ (*Step f*). This overall process is reversible in nature as shown by the deuterium enrichment at C(2) of both unreacted Q and THQ, as well as by HD formation. The 1,2-DHQ formed is a cyclic olefin and, as such, can be

Scheme 11

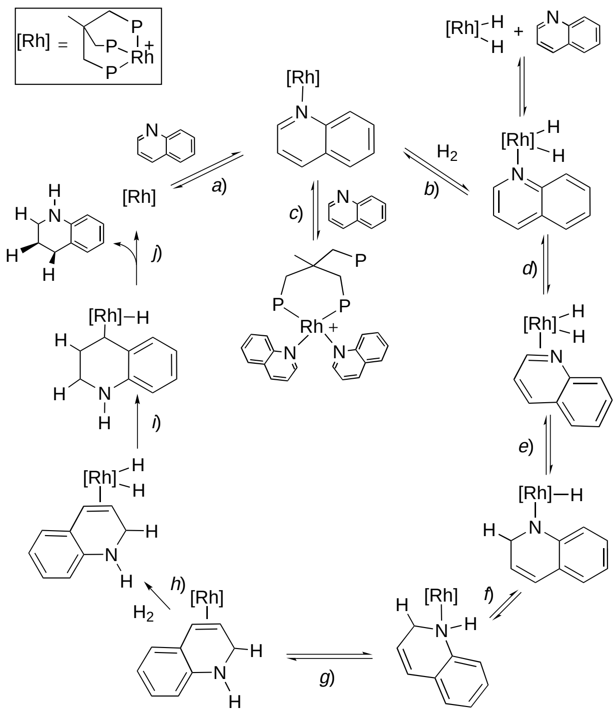

hydrogenated by the [Rh(triphos)]$^+$ system through a classical olefin hydrogenation mechanism (*Steps h–j*) [22]. No further deuterium enrichment, aside from the expected D-atoms at C(3) and C(4), was found, and, therefore, it can be concluded that the reduction of the C(3)=C(4) bond of 1,2-DHQ is irreversible in nature.

In the absence of a quantitative treatment of the kinetic data, the rate-limiting step can be identified only through a perusal of indirect experimental evidence. The first substantial indication that the rate-limiting step had to be sought in the conversion of Q to 1,2-DHQ was provided by the much faster rate of the irreversible hydrogenation of 1,2-DHQ to THQ in comparison with the overall transformation of Q into THQ. In standard catalytic conditions ([Q] $\leq$ 70 mM), the dihydride **7** is the largely predominant Rh complex (at least on the NMR time scale), and the rate is first-order in [Rh], [H_2], and [Q]. From a mechanistic viewpoint, this means that all the reactions involving the Rh complex, H_2, and Q should take place reversibly before or within the rate-determining step. The reversible migration of the hydride from Rh to C(2) (*Step e*), which also disrupts the aromaticity of the substrate, possesses all of these features and thus, in our opinion, is the best candidate for the rate-determining step.

The mechanism of reduction of Q to THQ by a homogeneous metal catalyst has been studied in a few cases only, which reflects the inherent difficulty of disrupting the aromaticity of N-heterocycles [7a][9e,c].

The mechanism proposed in *Scheme 11* shares some analogies with that reported by *Fish* and co-workers for the selective hydrogenation of Q to THQ in CH_2Cl_2 catalyzed by the Rh^{III} precursor $[Rh(MeCN)_3Cp^*]^{2+}$ (40°, 33 bar H_2) [7a]. Common features are the critical role of N-atom coordination for selective heterocycle reduction, the *cis*-deuteration of the C(2)–C(3) bond of Q, and the reversibility of the C(2)=N bond hydrogenation, which, in both systems, has been named the rate-determining step. Unlike the triphos-based catalyst, the Cp* system shows a reversible C(3)=C(4) bond reduction as well as Rh complexation to the carbocyclic ring resulting in C(6)–H and C(8)–H bond activation, which reflects the more sterically congested nature of triphos as compared to Cp*.

4. Conclusions. – In this and previous papers, we have investigated the hydrogenation of *N*- and *S*-heterocycles in the presence of homogeneous catalysts containing the *promoter* metals Rh and Ru supported by the tripodal ligand triphos. It has been found that the highly energetic C_s-symmetric $16e^-$ Rh^I and Ru^0 fragments [RhH(triphos)] and $[RuH(triphos)]^-$ insert into C–S bond of thiophenes, leading ultimately to catalytic hydrogenolysis to thiols [20c][21b,d,g] while they are inactive towards N-heterocycles. The much higher bond energy of C–N bonds as compared to C–S bonds (by 3–9 kcal mol^{-1}) certainly contributes to make C–N insertion much more difficult to accomplish than C–S insertion. On the other hand, the Rh and Ru electron-rich systems are also unable to catalyze the plain hydrogenation of N-heterocycles to cyclic amines. In our opinion, the *soft* character of the metal center in $[RuH(triphos)]^-$ and [RhH(triphos)] disfavors N-atom coordination that is crucial for the hydrogenation of N-heterocycles [3][7]. In contrast, the *soft* character of sulfur allows for the S-atom coordination of thiophenes, hence for C–S insertion, but disfavors the (2,3-η) coordination that is necessary for the selective hydrogenation of the heterocycle [20][21]. Consistent with this picture, catalysts containing *hard* metal ions, as in the Rh^{III} fragment $[Rh(H)_2(triphos)]^+$ and in the recently investigated Ru^{II} fragment $[RuH(triphos)]^+$ [20][21], are efficacious for the selective hydrogenation of both N-heterocycles and S-heterocycles due to their propensity to bind the former *via* N- and the latter *via* two C-atoms. The overall reactivity pattern for the prototypical substrates BT and Q is summarized in *Scheme 12*.

In conclusion, besides providing further mechanistic insight into the selective hydrogenation of the heterocyclic ring in Q, this study may contribute to rationalizations of why efficacious hydrotreating catalysts contain *component* and *promoter* metal sites in variable coordination numbers and oxidation states [1][3][19]. Such variability in chemical structure is actually needed to ensure the simultaneous reductive degradation of as many different types of heteroatoms as possible. A clear-cut rationalization of the relationship between the nature of the metal site and the reactivity of a specific heteroaromatic substrate is lacking in the relevant literature, and most of current improvements in catalyst composition are still achieved *via* trial-and-error procedures. Homogeneous model studies, like the present one, may be very useful to elucidate the structure/reactivity relationships by exploitation of the relative ease by which the molecular architecture of homogeneous catalysts can be tailored to meet the optimal steric and electronic requisites for either hydrogenation or hydrogenolysis of a specific substrate.

Scheme 12

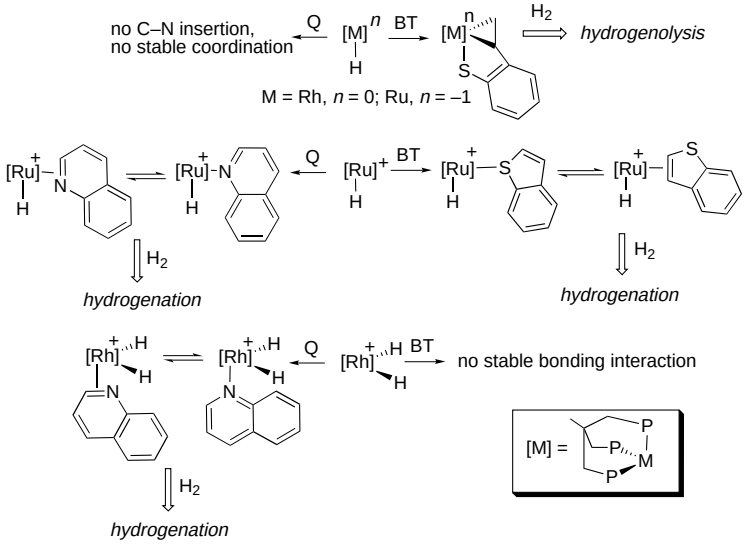

Thanks are due to *MURST* (Italy) for cofinancing this research (legge 95/95).

Experimental Part

General. All reactions and manipulations, except as stated otherwise, were routinely performed under N_2 with standard *Schlenk* techniques. Reactions under a controlled pressure of H_2 were performed with a stainless steel *Parr 4565* reactor (100 ml) equipped with a *Parr 4842* temperature and pressure controller. The reactor was connected to gas reservoir to maintain a constant pressure over the catalytic reactions. The Rh complexes [Rh(DMAD)(triphos)]PF_6 [22a], [Rh(S(C_6H_4)CH=CH_2-$\kappa^2C^{1',2'}$,κS)(triphos)] [21j], [RhH_3(triphos)] [24b], [RhCl(C_2H_4-κ^2C)(triphos)] [22a], [Rh(COD)(triphos)]PF_6 [38], [RhH(DMFU-$\kappa^2C^{2,3}$)(triphos)] [22b,c], and [RhCl$(H)_2$(triphos)] [22a] were prepared as previously described. The isolated metal complexes were collected on sintered-glass frits and washed with appropriate solvents before being dried under a stream of N_2. Q (98%, *Aldrich*) was purified by distillation under N_2. TfOH (98%), and TsOH·H_2O (98%) were purchased from *Aldrich* and used without further purification. 1,2-DHQ was prepared by reduction of Q with $LiAlH_4$ in diethyl ether according to [39]: [^{1}H-NMR ((D$_8$)THF, 20°, 200.13 MHz): 4.28 (*m*, CH_2); 4.82 (br., NH); 5.65 (*dtd*, *J*(CHCH′) = 9.8, *J*($CHCH_2$) = 3.8, *J*(CHNH) = 1.6, CH); 6.30 (*dt*, *J*(CH′CH) = 9.8, *J*(CH′CH_2) = 1.5, CH′); 6.3–7.0 (4 arom. H)]. The samples of 1,2-DHQ were invariably contaminated with some 1,4-DHQ (5–10%). THF and (D$_8$)THF were purified by distillation from $LiAlH_4$ under N_2. Deuterated solvents for NMR measurements were dried over molecular sieves. All of the other reagents and chemicals were reagent grade and used as received from commercial suppliers.

GC Analyses: *Shimadzu GC-14A* gas chromatograph equipped with a flame ionization detector and a 30 m (0.25 mm i.d., 0.25 μm film thickness) *SPB-1 Supelco* fused silica capillary column. IR Spectra: *Perkin-Elmer 1600* series FT-IR spectrophotometer; samples as Nujol mulls between KBr plates, ν in cm^{-1}. Routine ^{1}H- (200.13 MHz), ^{13}C{^{1}H}- (50.32 MHz), and ^{31}P{^{1}H}-NMR (81.01 MHz) spectra were obtained on a *Bruker ACP-200* spectrometer. All chemical shifts (δ) are reported in ppm relative to Me_4Si referenced to the chemical shifts of residual solvent resonances (^{1}H, ^{13}C) or 85% H_3PO_4 (^{31}P), with downfield values reported as positive. ^{31}P{^{1}H}- and ^{1}H-NMR experiments on compounds **6a**–**c** were recorded on either a *Bruker Avance DRX-500* spectrometer at 202.47 and 500.13 MHz, respectively, or a *Bruker Avance DRX-400* spectrometer at 161.98 and 400.132 MHz, respectively. Both instruments were equipped with variable-temp.-control units accurate to ± 0.1°. The assignments of the signals were based on 1D spectra, 2D ^{31}P{^{1}H}-COSY, ^{1}H-TOCSY, ^{1}H-NOESY, ^{1}H-

ROESY and proton-detected ^1H-^{31}P correlations performed on nonspinning samples. 2D NMR Spectra were recorded with pulse sequences suitable for phase-sensitive representations with TPPI. The $^{31}P\{^1H\}$-COSY spectrum was acquired at 161.98 MHz, whereas all the proton-detected 2D experiments were acquired at 500.13 MHz. The coupling constants were obtained from the 1D spectra and $^1H\{^{31}P\}$ heteronuclear decoupling experiments. Standard pulse sequences were used for the ^1H-TOCSY [40], ^1H-NOESY [41], ^1H-ROESY [42], and ^1H-^{31}P correlations [43]. In a typical experiment, 1024 increments of size 2K (with 16 scans each) covering the full range in both dimensions (*ca.* 6000 Hz for ^1H and *ca.* 13000 Hz for ^{31}P) were acquired with a relaxation delay of 2.0 sec. A TOCSY mixing time of 170 ms was used, whereas the NOESY mixing time and ROESY spin-lock time were 650 ms and 500 ms, resp. ^1H-^{31}P correlations optimized for the detection of $J(H,P)$ couplings of 5 and 15 Hz were recorded. The $^{31}P\{^1H\}$-COSY [44] spectrum was obtained with ^1H decoupling during acquisition: 1024 increments of size 2K (with 64 scans each) covering the full range in both dimensions (*ca.* 12000 Hz) were collected with a relaxation delay of 1.0 sec. For HP-NMR experiments, a 10-mm sapphire NMR tube (*Saphikon*, Milford, NH) was used, and the Ti high-pressure charging head was constructed at the ISSECC-CNR (Firenze, Italy) [45]. *Caution:* Since high gas pressures are involved, safety precautions must be taken at all stages of studies involving high-pressure NMR tubes. GC/MS Analyses: *Shimadzu QP-5000*; column identical to that used for GC analyses; *m*/*z* (%). Elemental analyses (C, H, N) were performed with a *Carlo-Erba Model 1106* elemental analyser. Atomic-absorption analyses were performed with a *Perkin-Elmer 5000* instrument.

Reaction of **1** *with* H_2 *in* $(D_8)THF$. A 10 mm sapphire tube was charged with a (D_8)THF (2 ml) soln. of **1** (22.3 mg, 0.022 mmol) under N_2. The tube was pressurized with H_2 to 30 bar at r.t. and then placed into a NMR probe at 20°. The reaction was followed by variable-temp. $^{31}P\{^1H\}$- and ^1H-HP-NMR spectroscopy. Selective hydrogenation occurred already at r.t., yielding DMSU (^1H-NMR: 3.72 (*s*, 2 MeO); 2.67 (*s*, 2 CH_2)) and the known THF adduct **3** [25]. Increasing the temp. to 40° led to the quantitative conversion of **1** to the binuclear compound **4** and, to a lesser extent, to the hydride containing triphos-Rh complex **5** ($^{31}P\{^1H\}$-NMR: 27.1 (*m*, P_A); 25.2 (*m*, P_M); 9.1 (*m*, P_Q). ^1H-NMR: −8.55 (*dm*, $J(H,P) = 153$, Rh−H)].

Catalytic Hydrogenation of Q (ca. 200 mM*) with the Catalyst Precursor* **1**. A 10 mm sapphire tube was charged with a (D_8)THF (2 ml) solu. of **1** (11 mg, 0.011 mmol) and a 40-fold excess of Q (25 µl, 0.44 mmol) under N_2. The tube was pressurized with H_2 to 30 bar at r.t. and then placed into a NMR probe at 20°. The reaction was followed by variable-temp. $^{31}P\{^1H\}$- and ^1H-HP-NMR spectroscopy. A sequence of selected $^{31}P\{^1H\}$-NMR spectra is reported in *Fig. 1*. The details of this investigation are discussed in a previous section. Transformation of **1** occurred at r.t. only in the presence of H_2 yielding the bis-Q complexes **6a**–**c**, as major products, accompanied by the dihydride **7** and the known fumarate-monohydride **8** [22b,c]. Occasionally, minor amounts of the phosphine oxide derivatives **6x**–**z** were detected in soln. Compounds **6a**–**c**, **6x**–**z**, and **7** were identified by comparison of their $^{31}P\{^1H\}$ and ^1H-NMR spectra with those of authentic specimens (see below). Selective reduction of Q to THQ occurred only after heating to 40°.

Catalytic Hydrogenation of Q (ca. 70 mM*) with* **1**. A 10 mm sapphire tube was charged with a (D_8)THF (2 ml) soln. of **1** (11 mg, 0.011 mmol) and a *ca.* 13-fold excess of Q (17 µl, 0.15 mmol) under N_2. The tube was pressurized with H_2 to 30 bar at r.t. and then placed into a NMR probe at 20°. The reaction was followed by variable-temp. $^{31}P\{^1H\}$- and ^1H-HPNMR spectroscopy. The spectra, immediately recorded at 20°, showed the conversion of **1** to the dihydride complex **7** and to the fumarate derivative **8**, as a minor species. Hydrogenation of Q to THQ already occurred at this temp. Increasing the temp. to 40° led to the conversion of **7** and **8** to the bis-Q derivatives **6a**–**c**/**6x**–**z** and also accelerated the hydrogenation of Q, which was complete in *ca.* 1 h. When all Q was hydrogenated, the hydride species **5** became the predominant Rh compound in soln.

Catalytic Hydrogenation of Q (ca. 30 mM*) with* **1**. A 10 mm sapphire tube was charged with a (D_8)THF (2 ml) soln. of **1** (11 mg, 0.011 mmol) and a *ca.* 5-fold excess of Q (7 µl, 0.06 mmol) under N_2. The tube was pressurized with H_2 to 30 bar at r.t. and then placed into a NMR probe at 20°. The reaction was followed by variable-temp. $^{31}P\{^1H\}$- and ^1H-HP-NMR spectroscopy. The hydrogenation of Q to THQ was almost complete within 30 min. In the meantime, **1** was rapidly converted to **7** and, to a much lesser extent, to **5**. When all Q was hydrogenated, only the hydride **5** was found in soln. During the course of the experiment, no formation of the bis-Q complexes was observed.

In Situ *NMR Study of the Catalytic Hydrogenation of 1,2-DHQ with the Catalyst Precursor* **1** *at the Same Catalyst and Substrate Concentrations as in the Autoclave Experiments.* In a typical NMR experiment, a 10 mm sapphire tube was charged with a (D_8)THF (2 ml) soln. of **1** (1.5 mg, $1.45 \cdot 10^{-3}$ mmol) and a 100-fold excess of 1,2-DHQ (17 µl, 1.45 mmol) under N_2 at r.t.. The tube was pressurized with H_2 to 30 bar and then placed into a NMR probe at r.t. (*ca.* 10 min after pressurization). The temp. of the probe was then increased to 60°. As soon as the temp. stabilized, ^1H-NMR spectra were acquired every 5 min. Under these experimental conditions, all 1,2-

DHQ disappeared to give a 3:1 mixture of THQ and Q within 10 min as a consequence of both disproportionation into Q and THQ, and hydrogenation to THQ. In an analogous experiment performed with Q as the starting substrate, 10% Q was hydrogenated in 10 min. Finally, when the NMR tube was charged with 100 equiv. of both Q and 1,2-DHQ, transformation of *ca.* 90% 1,2-DHQ occurred in 10 min. In all the experiments, the small quantity of 1,4-DHQ disappeared under H_2 already at r.t.

Attempted Catalytic Hydrogenation of Q with the Catalyst Precursor **2**. A 10 mm sapphire tube was charged with a (D_8)THF (2 ml) soln. of **2** (12 mg, 0.014 mmol) and Q (25 µl, 0.44 mmol) under N_2. The tube was pressurized with H_2 to 30 bar at r.t. and then placed into a NMR probe at r.t.. The reaction was followed by variable-temp. $^{31}P\{^1H\}$- and ^1H-HPNMR spectroscopy. No reaction occurred at temp. lower than 60°. At higher temp., the initially formed (*o*-ethylthiophenolate) dihydride complex [$Rh(H)_2(o\text{-}S(C_6H_4)C_2H_5)$(triphos)] [21g] underwent decomposition to several unknown species, as found in analogous experiments in performed THF alone [21a,f,g], without hydrogenation of Q.

Synthesis of **6a**–**c**. *NMR Experiments.* a) A 5 mm NMR tube was charged under N_2 at r.t. with a mixture of 30 mg of [$RhCl(\eta^2\text{-}C_2H_4)$(triphos)] (0.04 mmol) and 13 mg of $TlPF_6$ (0.04 mmol), and then with a (D_8)THF (0.9 ml) soln. of Q (18 ml, 0.16 mmol). The $^{31}P\{^1H\}$- and ^1H-NMR spectra of this sample showed the quantitative formation of **6a**–**c**. Occasionally, minor amounts of the phosphine oxide derivatives **6x**–**z** formed in soln.

b) A 5 mm NMR tube was charged under N_2 at r.t. first with 25 mg of [Rh(COD)(triphos)]PF_6 (0.026 mmol) and then with a CD_3OD (0.9 ml) soln. of Q (120 µl, 1 mmol). The tube was flame-sealed and then placed into a NMR probe at r.t.. The reaction was followed by variable-temp. $^{31}P\{^1H\}$- and ^1H-NMR spectroscopy. The starting Rh complex was found to convert to **6a**–**c** only when the probe head was heated to 100°; complete conversion occurred in *ca.* 1 h.

Oxidation of **6a**–**c** *to* **6x**–**z** *in Air*. Either air or O_2 (0.5 ml) was added by syringe to a soln. of **6a**–**c** (0.022 mmol) in (D_8)THF (0.9 ml) prepared as described above. The formation of **6x**–**z** was almost instantaneous and the complete transformation of **6a**–**c** occurred in *ca.* 30 min at r.t..

Reaction of **6a**–**c** *with* H_2. A 10 mm sapphire tube was charged with a (D_8)THF (2 ml) soln. of **6a**–**c** (0.022 mmol), pressurized with H_2 to 30 bar and then placed into a NMR probe at r.t. The reaction was followed by variable-temp. $^{31}P\{^1H\}$- and ^1H-HP-NMR spectroscopy. At 40°, **6a**–**c** were converted to **7** and THQ. With time, **7** decomposed to give a mixture of **4** and **5**.

Synthesis of **7**. To a soln. of [$RhCl(H)_2$(triphos)] (0.15 mg, 0.2 mmol) and Q (25 µl, 0.2 mmol) in 20 ml of THF was added 70 mg of $TlPF_6$ (0.2 mmol) under vigorous stirring. The mixture was allowed to stir for 1 h at r.t. After TlCl was removed by filtration, the resultant soln. was concentrated to half the volume under vacuum. Portionwise addition of heptane (40 ml) led to the precipitation of **7** as a pale yellow solid, which was filtered and washed with pentane, yield 70%. $^{31}P\{^1H\}$-NMR ((D_8)THF, 20°, 81.01 MHz): AM_2X spin system, 42.2 (*dt*, $J(P_M,P_A) = 23.4$, $J(P_M,Rh) = 77.9$, P_M); 13.5 (*dd*, $J(P_A,Rh) = 111.3$, P_A). ^1H-NMR ((D_8)THF, 20°, 200.13 MHz): −6.62 (second-order *dm*, $AA'XX'YZ$ spin system, $|{}^2J(H,P_M) + {}^2J(H,P_{M'})| = 160.3$, ${}^2J(H,P_A) = 12.1$, ${}^1J(H,Rh) = 8.5$, 2 Rh−H). Anal. calc. for $C_{50}H_{48}F_6NP_4Rh$: C 59.8, H 4.8, N 1.4; found: C 59.7, H 4.9, N 1.4.

Reaction of **1** *with* H_2 *in* (D_8)*THF in the Presence of TfOH.* A 10 mm sapphire tube was charged with a (D_8)THF (2 ml) soln. of **1** (22.3 mg, 0.022 mmol) and TfOH (6 µl, 0.07 mmol) under N_2. The tube was pressurized with H_2 to 30 bar at r.t. and then placed into a NMR probe at 20°. The reaction was followed by variable-temp. $^{31}P\{^1H\}$- and ^1H-HP-NMR spectroscopy. A sequence of selected $^{31}P\{^1H\}$-NMR spectra is reported in *Fig. 2*. Compound **1** was found to be converted to two rapidly interchanging monohydride complexes **11**/**12**, *ca.* 1:2. Details of this study are discussed in a previous section.

Data for **11**: ^1H-NMR (200.13 , 20°): −6.29 (*dq*, $J(H,P_{trans}) = 202.6$, $J(H,P_{cis}) = J(H,Rh) = 7.5$, Rh−H) (−30°): −6.23 (*dq*, $J(H,P_{trans}) = 196.2$, $J(H,P_{cis}) = J(H,Rh) = 7.8$, Rh−H). $^{31}P\{^1H\}$-NMR (81.01 MHz, 20°): AM_2X spin system; 42.1 (br., P_M); −12.3 (*dt*, $J(P_A,P_M) = 18.5$, $J(P_A,Rh) = 69.8$, P_A) (−30°): AM_2X spin system; 40.4 (*dd*, $J(P_M,P_A) = 20.1$, $J(P_M,Rh) = 122.6$, P_M); −11.5 (*dt*, $J(P_A,Rh) = 70.3$, P_A). *Data for* **12**: ^1H-NMR (200.13 MHz, 20°); −6.29 (*dq*, $J(H,P_{trans}) = 202.6$, $J(H,P_{cis}) = J(H,Rh) = 7.5$, Rh−H); (−30°): −6.15 (*dq*, $J(H,P_{trans}) = 195.3$, $J(H,P_{cis}) = J(H,Rh) = 7.4$, Rh−H). $^{31}P\{^1H\}$-NMR (81.01 MHz, 20°): AM_2X spin system; 42.1 (br., P_M); −12.3 (*dt*, $J(P_A,P_M) = 18.5$, $J(P_A,Rh) = 69.8$, P_A); (−30°): AMQX spin system; 47.9 (*ddd*, $J(P_A,P_M) = 41.4$, $J(P_A,P_Q) = 15.0$, $J(P_A,Rh) = 130.1$, P_A); 35.4 (*ddd*, $J(P_M,P_Q) = 23.6$, $J(P_MRh) = 121.5$, P_M); −12.8 (*dt*, $J(P_Q,Rh) = 72.0$, P_Q).

Reaction of **9** *with TfOH. a*) *NMR at 20°.* A *Teflon*-capped resealable 5 mm NMR tube was charged under N_2 at r.t. with a solid sample of **9** (30 mg, 0.04 mmol). A soln. of 1 equiv. of TfOH (7.5 µl, 0.04 mmol) in (D_8)THF (0.9 ml) was then introduced by syringe. The solid immediately dissolved, with gas evolution. $^{31}P\{^1H\}$- and ^1H-NMR spectra taken immediately after dissolution showed the formation of H_2 and the disappearance of **9**. Formed in its place were the dihydride complexes **3** as triflate salt and **10**, together with the monohydrides **11**

and **12** as minor species. Further addition of 1 equiv. of TfOH caused the conversion of the dihydride complexes to a mixture of **11** and **12**. Substitution of TsOH for TfOH yielded the monohydride complex [RhH(O-$SO_2(C_6H_4)$*p*-Me)$_2$(triphos)] analogous to **11**, while the use of $HBF_4 \cdot OEt_2$ led to the formation of dihydride intermediates, such as **3** as tetrafluoroborate salt, that decomposed to **4** $\mathbf{BF_4}$.

Data for **10**. ^{1}H-NMR (200.13 MHz): -6.52 (second-order *dm*, AA′XX′YZ spin system, $|^2J(H,P_M)+{}^2J(H,P_{M'})| = 179.6$, $^2J(H,P_A) = {}^1J(H,Rh) = 9.2$, 2 Rh–H). ^{31}P{^{1}H}-NMR (81.01 MHz): AM_2X spin system; 56.9 (*dt*, $J(P_A,P_M) = 22.5$, $J(P_A,Rh) = 150.2$, P_A); 2.1 (*dd*, $J(P_M,Rh) = 79.6$, P_M).

Data for [RhH($OSO_2(C_6H_4)$p-*Me)$_2$(triphos)]:* ^{1}H-NMR (200.13 MHz): -6.25 (*dq*, $J(H,P_{trans}) = 201.6$, $J(H,P_{cis}) = J(H,Rh) = 7.5$, Rh–H). ^{31}P{^{1}H}-NMR (81.01 MHz): AM_2X spin system; 43.2 (br., P_M); -14.1 (*dt*, P_A).

b) *NMR Experiment at* $-70°$. Neat TfOH (11 µl, 0.12 mmol) was added by syringe to a suspension of **9** (30 mg, 0.04 mmol) in (D_8)THF (0.9 ml) contained in a *Teflon*-capped resealable 5-mm NMR tube under N_2 at $-70°$. The tube was rapidly transferred into a NMR probe precooled to $-70°$. ^{31}P{^{1}H}- and ^{1}H-NMR spectra, immediately recorded at this temp., showed the quantitative conversion of **9** to the known nonclassical dihydrogen complex [$Rh(H)_2(\eta^2$-$H_2)$(triphos)](OSO_2CF_3) [25] and, to a much lesser extent, to the THF adduct **3** as triflate salt. Increasing the temp. to $-30°$ led to the complete conversion of the dihydrogen complex to **3** **OTf** and, as minor species, **11** and **12**. Within 60 min at this temp., the monohydride complexes **11** and **12** (1:2 ratio) became the only Rh species to be detected in soln.

Synthesis of **11**. Into a stirred suspension of **9** (250 mg, 0.34 mmol) in THF (20 ml) was added a soln. of TfOH (125 µl, 1.37 mmol) in THF (10 ml). The starting complex rapidly dissolved with H_2 evolution. After 30 min, the resultant yellow-brown soln. was conc. to *ca.* 5 ml *in vacuo*. Portionwise addition of heptane (5 × 3 ml) led to the precipitation of **11** as a microcrystalline pale yellow solid, which was filtered off and washed with pentane. Yield 75%. IR: 2026 (Rh–H). Anal. calc. for $C_{43}H_{40}F_6O_6P_3RhS_2$: C 50.3, H 3.9, Rh 10.0; found: C 50.5, H 4.0, Rh 9.8.

Reaction of **11** *with Q*. Into a 5-mm NMR tube containing a (D_8)THF (0.9 ml) soln. of **11** (22.6 mg, 0.022 mmol), 104 µl of Q (0.88 mmol) was added with a syringe at r.t. under N_2. The ^{31}P{^{1}H}- and ^{1}H-NMR spectra of this sample showed quant. formation of **6a–c** as triflate salts, somewhat contaminated with **6x–z**.

Catalytic Hydrogenation of Q with the Catalyst Precursor **1** *in the Presence of TfOH.* A 10-mm sapphire tube was charged with a (D_8)THF (2 ml) soln. of **1** (11 mg, 0.011 mmol), TfOH (10 µl, 0.11 mmol), and a 40-fold excess of Q (25 µl, 0.44 mmol) under N_2. The tube was pressurized with H_2 to 30 bar at r.t. and then placed into a NMR probe at 20°. The reaction was followed by variable-temp. ^{31}P{^{1}H}- and ^{1}H-HP-NMR spectroscopy. A sequence of selected ^{31}P{^{1}H}-NMR spectra is reported in *Fig. 3*. Transformation of **1** occurred at r.t. only in the presence of H_2 to give slowly the bis-Q complexes **6a–c** (*Fig. 3, b*). Increasing the temp. to 40° favored the conversion process. Within 1 h, all of **1** had disappeared (*Fig. 3, c*), and 50% Q had been selectively hydrogenated to THQ.

Catalytic Hydrogenation of Q. Autoclave Experiments. The reaction conditions and the results of these experiments have been collected in *Table 3*. In a typical experiment, a 30 ml soln. of THF containing 0.022 mmol of catalyst precursor, 2.2 mmol substrate, and the required amount of TfOH was introduced by suction into an autoclave. After pressurizing with H_2 to the desired pressure at r.t., the mixture was heated to the appropriate temp. and then immediately stirred (750 rpm). During the reaction, the pressure level was kept constant with a continuous feed of H_2 from a high-pressure gas reservoir. After the desired time, the reaction was stopped by cooling the autoclave to r.t., and the pressure was then released. The product composition was determined by GC analysis of the crude reaction mixture. In the runs performed in the presence of acid cocatalysts, the added amounts of acid were neutralized with THF/H_2O solutions of NaOH before carrying out the GC analysis. In selected runs, the final soln. was concentrated to dryness *in vacuo* and the residue was dissolved in (D_8)THF and studied by ^{1}H- and ^{31}P{^{1}H}-NMR spectroscopy.

Autoclave Kinetics Experiments. The catalytic runs were performed according to a procedure analogous to that reported above. The reaction conditions and the results of these experiments have been collected in *Table 4*. To measure the substrate concentration as a function of time, the reactions were sampled every 10 min by withdrawing a few µl of soln. through a liquid outlet valve connected with a dip needle-pipe. The samples were maintained at $-20°$ for GC analysis. Each run was repeated at least three times to ensure reproducibility of the results. Concentrations of dissolved H_2 were calculated on the basis of published solubility data [36].

Catalytic Deuteration of Q with the Catalyst Precursor **1**. A soln. of **1** (22.3 mg, 0.022 mmol) and Q (266 µl, 2.2 mmol) in THF (30 ml) was placed into the *Parr* autoclave reactor under N_2. The system was charged with 15 bar of D_2 and heated to 60° with stirring. After 1 h, the reactor was cooled to r.t. and the excess D_2 was vented. The contents of the reactor were transferred into a *Schlenk*-type flask. GC Analysis showed 39% conversion of

Q to THQ. The solvent was then evaporated under reduced pressure and the residue was redissolved in pentane and passed through a bed of silica (pentane) to remove the catalyst. The soln. was then concentrated to dryness and the product was found to contain D-enriched Q and (D_3)THQ by ^{1}H-, ^{2}H-, and ^{13}C{^{1}H}-NMR spectroscopy and GC/MS.

Residual Q. NMR Spectroscopy showed a 20% deuterium enrichment at the 2-position in the residual Q, which is in agreement with the relative abundance of the isotopic species Q and (D_1)Q (81 and 19%, respectively) determined by GC/MS. ^{1}H-NMR (CD_2Cl_2, 500.13 MHz): 8.99 (*dd*, *J*(2,3) = 4.2, *J*(2,4) = 1.6, 0.8 H, H−C(2)); 8.22 (*dd*, *J*(4,3) = 8.3, *J*(4,2) = 1.6, H−C(4)); 8.10 (*dd*, *J*(8,7) = 8.1, *J*(8,6) = 1.2, H−C(8)); 7.90 (*dd*, *J*(5,6) = 8.1, *J*(5,7) = 1.2, H−C(5)); 7.80 (*td*, *J*(7,6) = *J*(7,8) = 8.2, *J*(7,5) = 1.4, 0.9 H−C(7)); 7.63 (*td*, *J*(6,5) = *J*(6,7) = 8.1, *J*(6,8) = 1.1, H−C(6)); 7.45 (*dd*, *J*(3,2) = 4.2, *J*(3,4) = 8.3, H−C(3)). ^{2}H-NMR (CH_2Cl_2, 76.77 MHz): 8.99 (br. *s*, ^{2}H−C(2)). ^{13}C{^{1}H}-NMR (CD_2Cl_2, 125.77 MHz): 151.11 (*s* and *t*, *J*(CD) = 24.0, C(2)); 149.06 (*s*, C(8a)); 136.53 (*s*, C(4)); 130.07 (*s*, C(8)); 130.04 (*s*, C(7)); 128.97 (*s*, C(5a)); 128.52 (*s*, C(5)); 127.28 (*s*, C(6)); 121.81 (*s*, C(3)). GC/MS (EI): 129 (100), 130 (33), 131 (2).

(D_3)THQ. NMR Spectroscopy showed the presence of 1.1 D-atoms at C(2) and 1 D-atom each at C(3) and C(4). Consistently, GC/MS analysis gave *m*/*z* values corresponding to the isotopic species (D_3)THQ (89%), (D_4)THQ (11%). The N-atom was found to be undeuterated because of rapid H/D exchange due to contact with moisture during workup. ^{1}H-NMR (CD_2Cl_2, 500.13 MHz): 7.02 (*m*, H−C(5), H−C(7)); 6.65 (*td*, *J*(6,5) = *J*(6,7) = 7.3, *J*(6,8) = 1.2, H−C(6)); 6.52 (*dd*, *J*(8,7) = 7.8, *J*(8,6) = 1.2, H−C(8)); 3.31 (br. *m*, 0.9 H−C(2)); 2.79 (br. *m*, H−C(4)); 1.94 (br. *m*, H−C(3)). ^{2}H-NMR (CH_2Cl_2, 76.77 MHz): 3.31 (br. *s*, 1.1 ^{2}H−C(2)); 2.79 (br. *m*, ^{2}H−C(4)); 1.94 (br. *s*, ^{2}H−C(3)). ^{13}C{^{1}H}-NMR (CD_2Cl_2, 125.77 MHz): 145.76 (*s*, C(8a)); 130.01 (*s*, C(5)); 127.13 (*s*, C(7)); 121.89 (*s*, C(5a)); 117.19 (*s*, C(6)); 114.58 (*s*, C(8)); 42.10 (*t*, *J*(C(2),D) = 20.9, C(2)); 27.19 (*t*, *J*(C(4),D) = 19.6, C(4)); 22.33 (*t*, *J*(C(3),D) = 19.7, C(3)). GC/MS (EI): 136 (100), 137 (22), 138 (3).

REFERENCES

[1] a) H. Topsøe, B. S. Clausen, F. E. Massoth, 'Hydrotreating Catalysis', Springer-Verlag, Berlin Heidelberg, 1996; b) J. Scherzer, A. J. Gruia, 'Hydrocracking Science and Technology', Marcel Dekker, New York, 1996; c) C. N. Satterfield, 'Heterogeneous Catalysis in Industrial Practice', McGraw-Hill, New York, 1991.

[2] M. L. Occelli, R. Chianelli, 'Hydrotreating Technology for Pollution Control', Marcel Dekker, New York, 1996.

[3] a) M. J. Girgis, B. C. Gates, *Ind. Eng. Chem. Res.* **1991**, *30*, 2031; b) T. C. Ho, *Catal. Rev.- Sci. Eng*. **1988**, *30*, 117; c) R. M. Laine, *Catal. Rev.- Sci. Eng*. **1983**, *25*, 459; d) J. R. Katzer, R. Sivasubramanian, *Catal. Rev. - Sci. Eng*. **1979**, *20*, 155; e) B. C. Gates, J. R. Katzer, G. C. A Schuit, 'Chemistry of Catalytic Processes', McGraw-Hill, New York, 1979, Chap. 6.

[4] C. Bianchini, A. Meli, F. Vizza, *Eur. J. Inorg. Chem*. **2001**, 43.

[5] R. Prins, M. Jian, M. Flechsenhar, *Polyhedron* **1997**, 16, 3235.

[6] a) K. J. Weller, P. A. Fox, S. D. Gray, D. E. Wigley, *Polyhedron* **1997**, *16*, 3139; b) K. J. Weller, S. D. Gray, P. Briggs, D. E. Wigley, *Organometallics* **1995**, *14*, 5588; c) S. D. Gray, K. J. Weller, M. A. Bruck, P. Briggs, D. E. Wigley, *J. Am. Chem. Soc.* **1995**, *117*, 10678; d) S. D. Gray, D. P. Smith, M. A. Bruck, P. Briggs, D. E. Wigley, *J. Am. Chem. Soc.* **1992**, *114*, 5462.

[7] a) E. Baralt, S. J. Smith, J. Hurwitz, I. T. Horváth, R. H. Fish, *J. Am. Chem. Soc.* **1992**, *114,* 5187; b) R. H. Fish, H-S. Kim, R. H. Fong, *Organometallics* **1991**, *10*, 770; c) R. H. Fish, R. H. Fong, A. Than, E. Baralt, *Organometallics* **1991**, *10*, 1209; d) R. H. Fish, E. Baralt, H-S. Kim, *Organometallics* **1991**, *10*, 1965; e) R. H. Fish, J. N. Michaels, R. S. Moore, H. Heinemann, *J. Catal.* **1990**, *123*, 74; f) R. H. Fish, H-S. Kim, R. H. Fong, *Organometallics* **1989**, *8*, 1375; g) R. H. Fish, H-S. Kim, J. E. Babin, R. D. Adams, *Organometallics* **1988**, *7*, 2250; h) R. H. Fish, T.-J. Kim, J. L. Stewart, J. H. Bushweller, R. K. Rosen, J. W. Dupon, *Organometallics* **1986**, *5*, 2193; i) R. H. Fish, J. L. Tan, A. Thormodsen, *Organometallics* **1985**, *4*, 1743; j) R. H. Fish, A. D. Thormodsen, H. Heinemann, *J. Mol. Catal*. **1985**, *31*, 191; k) R. H. Fish, J. L. Tan, A. Thormodsen, *J. Org. Chem*. **1984**, 49, 4500; l) R. H. Fish, A. Thormodsen, G. A. D. Cremer, *J. Am. Chem. Soc.* **1982**, *104*, 5234.

[8] a) R. M. Laine, *New J. Chem*. **1987**, *11*, 543; b) A. Eisenstadt, C. M. Giandomenico, M. F. Frederick, R. M. Laine, *Organometallics* **1985**, *4*, 2033; c) R. M. Laine, *J. Mol. Catal.* **1983**, *21*, 119; d) R. M. Laine, D. W. Thomas, L. W. Cary, *J. Org. Chem.* **1979**, *44*, 4964.

[9] a) Y. Alvarado, M. Busolo, F. López-Linares, *J. Mol. Catal. A: Chem.* **1999**, *142*, 163; b) M. Rosales, J. Navarro, L. Sanchez, A. Gonzales, Y. Alvarado, R. Rubio, C. De la Cruz, T. Rajmankina, *Transition Met. Chem*. **1996**, *21*, 11; c) M. Rosales, Y. Alvarado, M. Boves, R. Rubio, H. Soscun, R. Sánchez-Delgado,

Transition Met. Chem. **1995**, *20*, 246; d) R. A. Sánchez-Delgado, *J. Mol. Catal.* **1994**, *86*, 287; e) R. A. Sánchez-Delgado, D. Rondón, A. Andriollo, V. Herrera, G. Martin, B. Chaudret, *Organometallics* **1993**, *12*, 4291; f) B. Chaudret, F. A. Jalón, M. Pérez-Manrique, F. Lahoz, F. J. Plou, R. Sánchez-Delgado, *New J. Chem*. **1990**, *14*, 331; g) R. A. Sánchez-Delgado, E. Gonzalez, *Polyhedron* **1989**, *8*, 1431.

[10] a) A. J. Deeming, M. J. Stchedroff, C. Whitaker, A. J. Arce, Y. De Sanctis, J. W. Steed, *J. Chem. Soc.*, *Dalton Trans.* **1999**, 3289; b) A. J. Arce, R. Machado, Y. De Sanctis, M. V. Capparelli, R. Atencio, J. Manzur, A. J. Deeming, *Organometallics* **1997**, *16*, 1735; c) A. J. Arce, J. Manzur, M. Marquez, Y. De Sanctis, A. J. Deeming, *J. Organomet. Chem.* **1991**, *412*, 177; d) A. J. Deeming, A. J. Arce, Y. De Sanctis, M. W. Day, K. I. Hardcastle, *Organometallics* **1989**, *8*, 1408; e) K. I. Hardcastle, H. Minassian, A. J. Arce, Y. De Sanctis, A. J. Deeming, *J. Organomet. Chem.* **1989**, *368*, 119.

[11] a) M. Rakowski DuBois, L. D. Vasquez, R. F. Ciancianelli, B. C. Noll, *Organometallics* **2000**, *19*, 3507; b) M. Rakowski DuBois, *Coord. Chem. Rev.* **1998**, *174*, 191; c) L. Vasquez, B. C. Noll, M. Rakowski DuBois, *Organometallics* **1998**, *17*, 976; d) S. Chen, B. C. Noll, L. Peslherbe, M. Rakowski DuBois, *Organometallics* **1997**, *16*, 1089; e) S. Chen, L. Vasquez, B. C. Noll, M. Rakowski DuBois, *Organometallics* **1997**, *16*, 1757; f) M. Rakowski DuBois, K. G. Parker, C. Ohman, B. C. Noll, *Organometallics* **1997**, *16*, 2325; g) S. Chen, V. Carperos, B. C. Noll, R. J. Swope, M. Rakowski DuBois, *Organometallics* **1995**, *14*, 1221; h) F. Kvietok, V. Allured, V. Carperos, M. Rakowski DuBois, *Organometallics* **1994**, *13*, 60.

[12] a) T. S. Kleckley, J. L. Bennett, P. T. Wolczanski, E. B. Lobkowsky, *J. Am. Chem. Soc.* **1997**, *119*, 247; b) K. J. Covert, D. R. Neithamer, M. C. Zonnevylle, R. E. LaPointe, C. Schaller, P. T. Wolczanski, *Inorg. Chem*. **1991**, *30*, 2494; c) D. R. Neithamer, L. Parkanyi, J. F. Mitchell, P. T. Wolczanski, *J. Am. Chem. Soc*. **1988**, *110*, 4421.

[13] a) D. P. Smith, J. R. Strickler, S. D. Gray, M. A. Bruck, R. S. Holmes, D. E. Wigley, *Organometallics* **1992**, *11*, 1275; b) J. R. Strickler, M. A. Bruck, D. E. Wigley., *J. Am. Chem. Soc*. **1990**, *112*, 2814.

[14] a) D. A. Vicic, W. D. Jones, *Organometallics* **1999**, *18*, 134; b) D. A. Vicic, W. D. Jones, *Organometallics* **1997**, *16*, 1912; c) W. D. Jones, L. Dong, A. W. Myers, *Organometallics* **1995**, *14*, 855; d) W. D. Jones, R. M. Chin, R. M., *J. Am. Chem. Soc.* **1994**, *116*, 19826; e) G. C. Hsu, W. P. Kosar, W. D. Jones, *Organometallics* **1994**, *13*, 385.

[15] N. Nelson, R. B. Levy, *J. Catal*. **1979**, *58*, 485.

[16] I. Jardine, F. J. McQuillin, *J. Chem. Soc. D* **1970**, 626.

[17] a) D. E. Páez, A. Andriollo, R. A. Sánchez-Delgado, N. Valencia, R. E. Galiasso, F. López-Linares, U.S. Pat. 5.958.223 to INTEVEP S.A., 1999; b) D. E. Páez, A. Andriollo, R. A. Sánchez-Delgado, N. Valencia, F. López-Linares, R. E. Galiasso, U.S. Pat. 5.753.584 to INTEVEP S.A., 1998; c) D. E. Páez, A. Andriollo, F. López-Linares, R. E. Galiasso, J. A. Revete, R. A. Sánchez-Delgado, A. Fuentes, *Am. Chem. Soc. Div. Fuel Chem. Symp. Prepr*. **1998**, *43*, 563.

[18] C. Bianchini, M. Frediani, G. Mantovani, F. Vizza, *Organometallics* **2001**, *20*, 2660.

[19] a) C. Bianchini, A. Meli in 'Transition Metal Sulphides – Chemistry and Catalysis', Eds. T. Weber, R. Prins, R. A. van Santen, Kluwer, Dordrecht, 1998, p. 129; b) C. Bianchini, A. Meli, *Acc. Chem. Res.* **1998**, *31*, 109; c) C. Bianchini, A. Meli in 'Aqueous-Phase Organometallic Catalysis – Concepts and Applications', Eds.: B. Cornils, W. A. Herrmann, VCH, Weinheim, 1998, p. 477; d) Bianchini, A. Meli in 'Applied Homogeneous Catalysis with Organometallic Compounds', Eds.: B. Cornils, W. A. Herrmann, VCH, Weinheim, 1996, Vol. 2, p. 969; e) C. Bianchini, A. Meli, *J. Chem. Soc.*, *Dalton Trans.* **1996**, 801.

[20] a) C. Bianchini, A. Meli, S. Moneti, W. Oberhauser, F. Vizza, V. Herrera, A. Fuentes, R. A. Sánchez-Delgado, *J. Am. Chem. Soc*. **1999**, *121*, 7071; b) C. Bianchini, D. Masi, A. Meli, M. Peruzzini, F. Vizza, F. Zanobini, *Organometallics* **1998**, *17*, 2495; c) C. Bianchini, A. Meli, S. Moneti, F. Vizza, *Organometallics* **1998**, *17*, 2636.

[21] a) C. Bianchini, M. V. Jiménez, A. Meli, S. Moneti, V. Patinec, F. Vizza, *Organometallics* **1997**, *16*, 5696; b) C. Bianchini, A. Meli, V. Patinec, V. Sernau, F. Vizza, *J. Am. Chem. Soc*. **1997**, *119*, 4945; c) C. Bianchini, A. Meli, W. Pohl, F. Vizza, G. Barbarella, *Organometallics* **1997**, *16*, 1517; d) C. Bianchini, J. A. Casares, A. Meli, V. Sernau, F. Vizza, R. A. Sánchez-Delgado, *Polyhedron* **1997**, *16*, 3099; e) C. Bianchini, D. Fabbri, S. Gladiali, A. Meli, W. Pohl, F. Vizza, *Organometallics* **1996**, *15*, 4604; f) C. Bianchini, M. V. Jiménez, C. Mealli, A. Meli, S. Moneti, V. Patinec, F. Vizza, *Angew. Chem.*, *Int. Ed.* **1996**, *35*, 1706; g) C. Bianchini, V. Herrera, M. V. Jiménez, A. Meli, R. A. Sánchez-Delgado, F. Vizza, *J. Am. Chem. Soc*. **1995**, *117*, 8567; h) C. Bianchini, M. V. Jiménez, A. Meli, F. Vizza, *Organometallics* **1995**, *14*, 3196; i) C. Bianchini, M. V. Jiménez, A. Meli, F. Vizza, *Organometallics* **1995**, *14*, 4858; j) C. Bianchini, P. Frediani, V. Herrera, M. V. Jiménez, A. Meli, L. Rincon, R. A. Sánchez-Delgado, F. Vizza, *J. Am. Chem. Soc*. **1995**, *117*, 4333.

[22] a) C. Bianchini, A. Meli, M. Peruzzini, F. Vizza, *Organometallics* **1990**, *9*, 226; b) C. Bianchini, A. Meli, M. Peruzzini, F. Vizza, *Organometallics* **1990**, *9*, 2283; c) C. Bianchini, F. Laschi, A. Meli, M. Peruzzini, P. Zanello, P. Frediani, *Organometallics* **1988**, *7*, 2575.
[23] a) C. Bianchini, A. Meli, F. Laschi, J. A. Ramirez, P. Zanello, A. Vacca, *Inorg. Chem.* **1988**, *27*, 4429; b) C. Bianchini, A. Meli, P. Zanello, *J. Chem. Soc., Chem. Commun.* **1986**, 628; c) C. Bianchini, C. Mealli, A. Meli, M. Sabat, *J. Chem. Soc., Chem. Commun.* **1986**, 777.
[24] a) G. Kiss, I. T. Horvath, *Organometallics* **1991**, *10*, 3798; b) J. Ott, L. M. Venanzi, C. A. Ghilardi, S. Midollini, A. Orlandini, *J. Organomet. Chem*. **1985**, *291*, 89.
[25] V. I. Bakhmutov, C. Bianchini, M. Peruzzini, F. Vizza, E. V. Vorontsov, *Inorg. Chem.* **2000**, *39*, 1655.
[26] E. G. Thaler, K. G. Caulton, *Organometallics* **1990**, *9*, 1871.
[27] A. L. Crumbliss, R. J. Topping, in 'Phosphorus-31 NMR Spectroscopy in Stereochemical Analysis', Eds. J. G. Verkade, L. D. Quin, VCH, Weinheim, Germany, 1987, Chapter 15, p. 531.
[28] P. S. Pregosin, R. W. Kunz, '^{31}P and ^{13}C NMR of Transition Metal Phosphine Complexes', Ed. P. Diehl, E. Fluck, R. Kosfeld, Springer-Verlag, Berlin, 1979.
[29] P. A. MacNeil, N. K. Roberts, B. Bosnich, *J. Am. Chem. Soc.* **1981**, *103*, 2273; J. Bakos, I. Tóth, B. Heil, G. Szalontai, L. Párkányi, V. Fülöp, *J. Organomet. Chem.* **1989**, *370*, 263.
[30] C. Bianchini, H. M. Lee, P. Barbaro, A. Meli, S. Moneti, F. Vizza, *New J. Chem.* **1999**, *23*, 929.
[31] W. McFarlane, J. D. Swarbrick, J. L. Bookham, *J. Chem. Soc., Dalton Trans.* **1998**, 3233.
[32] P. S. Pregosin, R. Salzmann, A. Togni, *Organometallics* **1995**, *14*, 842.
[33] H. Berger, R. Nesper, P. S. Pregosin, H. Rügger, M. Wörle, *Helv. Chim. Acta* **1993**, *76*, 1520.
[34] A. Bax, 'Two-Dimensional Nuclear Magnetic Resonance in Liquids'; Delft University Press, Dordrecht, Holland, 1982.
[35] I. Goljer, P. H. Bolton, in 'Two-Dimensional NMR Spectroscopy, Application for Chemists and Biochemists', Ed. W. R. Croasmun, R. M. K. Carlson, VCH, New York, 1994.
[36] E. Brunner, *J. Chem. Eng. Data* **1985**, *30*, 269; C. L. Young, 'Solubility Data Series IUPAC', Pergamon Press, Oxford, 1981, Vol. 516, p 219; R. Battino, H. L. Clever, *Chem Rev.* **1966**, *66*, 395.
[37] C. Bianchini, H. M. Lee, A. Meli, F. Vizza, *Organometallics* **2000**, *19*, 849, and refs. therein.
[38] F. Bachechi, J. Ott, L. M. Venanzi, *Acta Cryst.* **1989**, *C45*, 724.
[39] K. W. Rosenmund, F. Zymalkowski, *Chem. Ber.* **1953**, *86*, 37.
[40] A. Bax, D. G. Davis, *J. Magn. Reson.* **1985**, *65*, 355.
[41] V. Sklener, H. Miyashiro, G. Zon, H. T. Miles, A. Bax, *FEBS Lett.* **1986**, *208*, 94; J. Jeener, B. H. Meier, P. Bachmann, R. R. Ernst, *J. Chem. Phys.* **1979**, *71*, 4546.
[42] A. Bax, D. G. Davis, *J. Magn. Reson.* **1985**, *63*, 207.
[43] A. Bax, R. H. Griffey, B. L. Hawkins, *J. Magn. Reson.* **1983**, *55*, 301.
[44] W. P. Aue, E. Bartholdi, R. R. Ernst, *J. Magn. Reson.* **1976**, *64*, 2229.
[45] C. Bianchini, A. Meli, A. Traversi, Ital. Pat. FI A000025, 1997.

Received March 30, 2001